THE JOURNAL OF BIOLOGICAL CHEMISTRY VOL. 285, NO. 47, pp. 36721–36735, November 19, 2010
Printed in the U.S.A.

Hyaluronan-CD44 Interaction Promotes c-Src-mediated Twist Signaling, MicroRNA-10b Expression, and RhoA/RhoC Up-regulation, Leading to Rho-kinase-associated Cytoskeleton Activation and Breast Tumor Cell Invasion*

Received for publication, July 7, 2010, and in revised form, August 19, 2010 Published, JBC Papers in Press, September 15, 2010, DOI 10.1074/jbc.M110.162305

Lilly Y. W. Bourguignon[1], **Gabriel Wong, Christine Earle, Katherine Krueger, and Christina C. Spevak**

From the Department of Medicine, Endocrine Unit (111N), University of California at San Francisco and Veterans Affairs Medical Center, San Francisco, California 94121

Dysregulation of microRNAs is observed in many cancers, including breast cancer. In particular, miR-10b appears to play an important role in tumor cell invasion and breast cancer progression. In this study, we investigated hyaluronan (HA)-induced CD44 (a primary HA receptor) interaction with c-Src kinase and the transcriptional factor, Twist, in breast tumor cells (MDA-MB-231 cells). Our results indicate that HA binding to CD44 promotes c-Src kinase activation, which, in turn, increases Twist phosphorylation, leading to the nuclear translocation of Twist and transcriptional activation. Further analyses reveal that miR-10b is controlled by an upstream promoter containing the Twist binding site(s), whereas ChIP assays demonstrate that stimulation of miR-10b expression by HA/CD44-activated c-Src is Twist-dependent in breast tumor cells. This process results in the reduction of a tumor suppressor protein (HOXD10), RhoA/RhoC up-regulation, Rho-kinase (ROK) activation, and breast tumor cell invasion. Treatment of MDA-MB-231 cells with PP2 (a c-Src inhibitor) or Twist-specific siRNAs effectively blocks HA-mediated Twist signaling events, abrogates miR-10b production, and increases HOXD10 expression. Subsequently, this c-Src/Twist signaling inhibition causes down-regulation of RhoA/RhoC expression and impairment of ROK-regulated cytoskeleton function (*e.g.* tumor cell invasion). To further evaluate the role of miR-10b in RhoGTPase signaling, MDA-MB-231 cells were also transfected with a specific anti-miR-10b inhibitor in order to silence miR-10b expression and block its target functions. Our results demonstrate that anti-miR-10b inhibitor not only enhances HOXD10 expression but also abrogates HA/CD44-mediated tumor cell behaviors in breast tumor cells. Taken together, these findings indicate that the HA-induced CD44 interaction with c-Src-activated Twist plays a pivotal role in miR-10b production, leading to the down-regulation of tumor suppressor protein (HOXD10), RhoGTPase-ROK activation, and tumor cell invasion. All of these events are critical prerequisite steps for the acquisition of metastatic properties by human breast cancer cells.

CD44 denotes a family of cell surface glycoprotein receptors that are expressed in a variety of human solid neoplasms, particularly those classified as breast cancer (1–16). Nucleotide sequence analyses reveal that many CD44 isoforms (derived by alternative splicing mechanisms) are variants of the standard form, CD44s (17). The presence of high levels of CD44 variant (CD44v) isoforms is emerging as an important metastatic tumor marker in a number of cancers, including human breast cancers (1–16). Recent studies have shown that CD44 is also expressed in tumor stem cells that have the unique ability to initiate tumor cell-specific properties (18). In fact, CD44 appears to be an important surface marker for cancer stem cells (18). Hyaluronan (HA)[2] (a major component in the extracellular matrix of most mammalian tissues) is also rich in stem cell niches (19). All CD44 isoforms contain an HA-binding site in their extracellular domain and thereby serve as a major cell surface receptor for HA (1–16). Importantly, both CD44 and HA are overexpressed/elevated at sites of tumor attachment (1–16). HA binding to CD44 not only affects cell adhesion to the matrix components but also is involved in the stimulation of a variety of tumor cell-specific functions leading to breast cancer progression (1–16).

The Src family kinases are classified as oncogenic proteins due to their ability to activate cell proliferation, spreading, and migration in many cell types, including epithelial tumor cells (20). It has been observed that the interaction between Src kinase and membrane-linked molecules regulates receptor signaling and various cellular functions (21). In fact, CD44-mediated cellular signaling has been determined to involve Src kinase family members (2, 15, 22). Moreover, the cytoplasmic domain of CD44 binds to c-Src kinase at a single site with high affinity (15). Most importantly, HA interaction with CD44 stimulates c-Src kinase activity, which, in turn, increases tyrosine phosphorylation of the cytoskeletal protein, cortactin. Subsequently, tyrosine phosphorylation of cortactin attenuates its ability to cross-link filamentous actin *in vitro* (15). Collec-

* This work was supported, in whole or in part, by National Institutes of Health Grants R01 CA66163, R01 CA78633, and P01 AR39448. This work was also supported by a Veterans Affairs merit review grant.

[1] A Veterans Affairs Senior Research Career Scientist. To whom correspondence and reprint requests should be addressed: Endocrine Unit (111N), Dept. of Medicine, University of California at San Francisco and Veterans Affairs Medical Center, 4150 Clement St., San Francisco, CA 94121. Tel.: 415-221-4810 (ext. 3321); Fax: 415-383-1638; E-mail: lilly.bourguignon@ucsf.edu.

[2] The abbreviations used are: HA, hyaluronan; ROK, Rho-kinase or Rho-binding kinase; miRNA, microRNA; MBS, myosin-binding subunit of myosin phosphatase.

tively, all of these observations support the notion that c-Src kinases participate in HA/CD44-mediated cellular events.

Members of the Rho subclass of the Ras superfamily (small molecular weight RhoGTPases (*e.g.* RhoA and RhoC)) are known to transduce signals regulating many cellular processes (23). Overexpression of certain RhoGTPases in human tumors often correlates with a poor prognosis (24–26). In particular, coordinated RhoGTPase signaling is considered to be part of a likely mechanism underlying tumor cell invasion, an obvious prerequisite for metastasis (24–27). A number of studies indicate that HA/CD44-mediated tumor cell-specific phenotypes are closely linked to cytoskeletal functions that involve the small GTP-binding proteins, such as RhoA/RhoC, Rac1, and Cdc42. Activation of RhoGTPase has been shown to produce specific structural changes in actin assembly, cytoskeleton reorganization, and tumor cell migration and invasion (23). Several different enzymes have been identified as possible downstream targets for RhoGTPases (*e.g.* RhoA and RhoC) during the regulation of cytoskeleton-mediated cell motility (24–27). One such enzyme is Rho-kinase (ROK; also called Rho-binding kinase), which is a serine-threonine kinase (11, 12, 28–32). ROK interacts with RhoA/RhoC in a GTP-dependent manner and phosphorylates a number of cellular proteins (11, 12, 28–32). For example, ROK phosphorylates myosin phosphatase and myosin light chain (30, 31), thereby activating myosin adenosine triphosphatase (ATPase) and generating actomyosin-mediated membrane motility (30, 31). However, the cellular and molecular mechanisms regulating the ability of Rho-activated ROK to cause CD44-positive breast tumor cells to migrate and invade other tissues remain poorly understood.

MicroRNAs (miRNAs) are endogenous small regulatory RNAs (~22 nucleotides) that control gene expression by repressing the translation and/or enhancing the degradation of target mRNAs through a process known as RNA interference (33). Recently, miRNA expression profiles have been utilized to define different types of cancers, including breast cancer (34, 35). In current studies, miRNA-10b was found to be overexpressed in malignant glioma in addition to the overexpression of RhoC and urokinase-type plasminogen activator receptor, which are contributors to glioma invasion and migration (36). Furthermore, in human esophageal cancer cell lines, KLF4 (Kruppel-like factor 4), a zinc finger protein that has been identified in several human tumors, is also a direct target of miR-10b (37). Moreover, cell invasion and metastasis were both shown to be initiated by miRNA-10b in breast cancer (38). A previous report showed that silencing of miR-10b with antagomirs (an anti-miR-10 inhibitor) both *in vitro* and *in vivo* significantly decreases the amount of miR-10b and the level of a functionally important miR-10b target, HOXD10, resulting in decreased metastasis (39). Thus, the miR-10b inhibitor appears to be a promising candidate for the development of new anti-metastasis agents.

Twist, a basic helix-loop-helix transcription factor protein, was initially identified as a major regulator of embryonic morphogenesis (40). It often dimerizes with other basic helix-loop-helix proteins, binds to short conserved sequences called E-boxes (5′-CANNTG-3′) in the promoter regions, and transcriptionally regulates target genes (41). A recent study indicates that activated c-Src kinase induces Twist expression at both the mRNA and protein levels (42). Elevated Twist expression is closely associated with angiogenesis and tumor metastasis (43). Overexpression of Twist in CD44-positive breast tumor cells promotes the generation of a breast cancer stem cell phenotype (44). Twist has also been shown to induce miR-10b, which inhibits the mRNA of HOXD10 and results in the increase of RhoC (38). Therefore, Twist has a definitive role in cancer progression. Understanding the mechanisms involved in Twist signaling and the subsequent expression of miR-10b is critically important for elucidating the mechanisms involved in HA/CD44-associated breast cancer metastasis.

In this study, we have discovered a new HA/CD44-mediated signaling mechanism that regulates Twist-associated miR-10b production. Our results indicate that HA/CD44-activated c-Src stimulates Twist phosphorylation, which, in turn, stimulates Twist-regulated miR-10b production. These events lead to the reduction of the tumor suppressor protein, HOXD10, RhoA/RhoC overexpression, ROK activation, and breast tumor cell invasion. Inhibition of either c-Src/Twist signaling or silencing miR-10b expression/function not only results in HOXD10 upregulation but also causes a reduction of RhoA/RhoC expression and an inhibition of ROK-mediated breast tumor cell invasion. Our findings strongly support the contention that c-Src, Twist, and miR-10b form a functional signaling axis that regulates RhoGTPase-ROK function and cytoskeleton-associated breast cancer metastasis.

MATERIALS AND METHODS

Cell Culture—The breast tumor cell line (MDA-MB-231 cells) was obtained from the American Type Culture Collection and grown in Eagle's minimum essential medium supplemented with Earle's salt solution, essential and non-essential amino acids, vitamins, and 10% fetal bovine serum.

Antibodies and Reagents—Monoclonal rat anti-CD44 antibody (clone 020; isotype IgG_{2b}; obtained from CMB-TECH, Inc., San Francisco, CA) recognizes a determinant of the HA-binding region common to CD44 and its principal variant isoforms (29, 45–47). This rat anti-CD44 was routinely used for HA-related blocking experiments and immunoprecipitation. Immunoreagents, such as mouse anti-phospho-c-Src antibody, mouse anti-lamin A/C antibody, rabbit anti-HOXD10 antibody, rabbit anti-RhoA antibody, goat anti-RhoC antibody, goat anti-ROK antibody, and goat anti-actin antibody were purchased from Santa Cruz Biotechnology, Inc. (Santa Cruz, CA). Other immunoreagents, such as rabbit anti-Twist antibody and rabbit anti-phosphotyrosine antibody, were purchased from Abcam Inc. (Cambridge, MA) and Millipore Corp. (Billerica, MA), respectively.

Healon HA polymers (~400,000–500,000 Da; purchased from Amersham Biosciences and The Upjohn Co.) were prepared by gel filtration column chromatography using a Sephacryl S1000 column. The purity of the HA polymers used in our experiments was further verified by anion exchange high performance liquid chromatography (HPLC), followed by protein and endotoxin analyses using a BCA protein assay kit (Pierce) and an *in vitro* limulus amebocyte lysate assay (Cambrex Bio Science Walkersville Inc., Walkersville, MD), respec-

tively. No protein or endotoxin contamination were detected in this HA preparation.

HA Profile Assays—The MDA-MB-231 cells were metabolically labeled with 100 μCi/ml [^{3}H]glucosamine (Amersham Biosciences) for 18 h and subsequently rinsed with Hanks' balanced salt solution 2–3 times. The medium and washes were combined, collected, and digested with proteinase K (50 μg/ml) at 60 °C for 4 h and heated at 100 °C for 10 min, followed by centrifugation at 15,000 × *g* for 15 min. The supernatants were then precipitated with ethanol, analyzed for HA size distribution using 1 × 30-cm Sephacryl S-400 column chromatography (Amersham Biosciences), and eluted with a solution containing 0.15 M sodium acetate, 0.1% CHAPS (pH 6.8) as described previously (29). Fractions of 0.5 ml were collected. The amount of radioactivity associated with each fraction was determined by scintillation counting. Some fractions were also used to test for their ability to bind to HA-binding protein-coated beads and/or to be digested by PH20 hyaluronidase.

Twist siRNA Preparation and Transfection—The siRNA sequence targeting human Twist (from mRNA sequence GenBank™ accession number NM_000474) corresponds to the coding region relative to the first nucleotide of the start codon. Target sequences were selected, using methodologies from the *Silencer* siRNA construction kit (Ambion). As recommended by Ambion, Twist1-specific targeted regions were selected beginning 50–100 nucleotides downstream from the start codon. Sequences close to 50% G/C content were chosen. Human TWIST-specific target sequences (target 1, AACAGCGAGGAAGAGCCAGAC; target 2, AAGCGGCGCAGCAGCAGGCGC; target 3, AAGAAGTCTGCGGGCTGTGGC; target 4, AAGATGGCAAGCTGCAGCTAT) and scrambled sequences were used. MDA-MB-231 cells were then transfected with siRNA using Lipofectamine 2000 (Invitrogen) according to the manufacturer's instructions. Cells were incubated with 50 pmol of siRNA containing scrambled sequences or no siRNA for at least 24 h before biochemical experiments.

Anti-miR-10b Inhibitor Preparation and Transfection—Anti-miR targeting miR-10b (anti-miR-10b inhibitor) (Ambion) and its corresponding negative control were transfected into MDA-MB-231 cells, using Lipofectamine 2000 reagent (Invitrogen) for 24 h. Cells were then treated with HA (50 μg/ml) (or no HA) for various time intervals (*e.g.* 0, 5 min, 10 min, 15 min, 30 min, 2 h, or 24 h) at 37 °C. The final concentrations of anti-miR-10b and miRNA-negative control used in experiments were 30 nM.

RNase Protection Assay for Detecting Mature miRNAs—Total RNA was isolated and enriched with the *miRvana* miRNA isolation kit (Ambion) from the human breast tumor cell line MDA-MB-231. The cells were untreated or pretreated with anti-CD44 antibody or transfected with Twist siRNA with a scrambled sequence, anti-miR-10b inhibitor, or miRNA-negative control in the presence or absence of HA. The c-Src inhibitor PP2 (5 μM) was also added to the cells. RNA concentrations were verified by measuring absorbance (A_{260}) on a NanoDrop Spectrophotometer ND-1000 (NanoDrop). The *mirVana* probe construction kit (Ambion) was used to synthesize the ^{32}P-labeled miR-10b antisense probe and miR-191 probe loading control according to the manufacturer's instructions (Ambion). Probes were then gel-purified using a 12% acrylamide, 8 M urea gel prior to hybridization experiments. The enriched small RNAs (1 μg) were added to the probe hybridization buffer in addition to the radioactive probe and RNase protection was then carried out using the *mirVana* miRNA detection kit (Ambion) according to the manufacturer's instructions. The denaturing gel was visualized using autoradiography. All samples were treated under similar conditions, and an additional radioactively labeled probe, miR-191, was used as a loading control.

Immunoprecipitation and Immunoblotting Techniques—MDA-MB-231 cells (untreated or pretreated with anti-CD44 antibody or a c-Src inhibitor, PP2 (5 μM) or transfected with Twist siRNA, scrambled siRNA, anti-miR-10b inhibitor, or miRNA-negative control) followed by HA (50 μg/ml) addition (or no HA addition) for various time intervals (*e.g.* 0, 5 min, 10 min, 15 min, 30 min, or 24 h) at 37 °C were immunoblotted using various immunoreagents (*e.g.* rabbit anti-HOXD10 (2 μg/ml), rabbit anti-RhoA (2 μg/ml), rabbit anti-RhoC (2 μg/ml), or goat anti-actin (2 μg/ml) (as a loading control), respectively). In addition, immunoprecipitation was conducted after homogenization of the cell lysate using rat anti-CD44 antibody followed by goat anti-rat IgG-beads. Subsequently, the immunoprecipitated materials were solubilized in SDS sample buffer, electrophoresed, and blotted onto nitrocellulose. After blocking nonspecific sites with 3% bovine serum albumin, the nitrocellulose filters were incubated with rabbit anti-phospho-c-Src antibody (2 μg/ml) or rabbit anti-Twist antibody (2 μg/ml) for 1 h at room temperature. In some cases, the cell lysates were immunoprecipitated with anti-Twist antibody, followed by goat anti-rabbit IgG-beads. Subsequently, the immunoprecipitated materials were processed for immunoblotting using rabbit anti-phosphotyrosine antibody (2 μg/ml). In certain experiments, the nuclear fraction prepared by an extraction kit from Active Motif (Carlsbad, CA) of MDA-MB-231 cells (untreated or pretreated with anti-CD44 antibody or PP2 (5 μM)) plus 50 μg/ml HA (or no HA) for various time intervals (*e.g.* 0, 5, 15, or 30 min) at 37 °C was immunoblotted with anti-Twist antibody or anti-lamin A/C, respectively.

Chromatin Immunoprecipitation (ChIP) Assay—Twist, a basic helix-loop-helix transcription factor, recognizes E-box elements of the canonical sequence 5′-CANNTG-3′. Several predicted E-box elements are located upstream of miR-10b (38), and ChIP assays were carried out to investigate whether Twist proteins bind to these E-boxes following HA treatment. Specific primers were designed to amplify a genomic region flanking a putative E-box directly upstream of miR-10b. Primer sequences are 5′-ACCTGGCTTGGTCGGGCAGT-3′ and 5′-CGCAGCCACCCGCACTTTCT-3′. These primers gave a single strong band when tested on input DNA. ChIP assays were carried out using the ChIP assay kit (Millipore Corp.) essentially according to the manufacturer's protocol. MDA-MD-231 cells (untreated or pretreated with anti-CD44 antibody or PP2 (5 μM)) plus 50 μg/ml HA (or no HA) for various time intervals (*e.g.* 0, 5, 15, 30, or 60 min) at 37 °C were fixed with 1% formaldehyde for 15 min, followed by a 5-min treatment with 1.25 M glycine to quench the reaction. Cell lysates were then sonicated to shear DNA in fragments 300 – 800 bp

in size. Precleared lysates were subjected to overnight immunoprecipitation with rabbit anti-Twist antibody (10 μg/ml) or normal rabbit IgG (10 μg/ml) (negative control). DNA samples were purified by phenol/chloroform extraction. Between 5 and 10 ng of immunoprecipitated DNA was used for PCRs. Preimmunoprecipitated samples (input) were also included as controls for PCR.

Luciferase Reporter Assay—To test the mechanisms by which HA treatment regulates miR-10b transcription, luciferase assays were performed. A 1.2-kb fragment containing the putative miR-10b promoter (48) and an E-box (38) was PCR-amplified from human genomic DNA using the following primers: 5′-tttacgcgtTGGGCAGTTGAGCGGGAGGT-3; 5′-tttagatctACGCAGCCACCCGCACTTTC-3′. The PCR product was digested with MluI and BglII (sites underlined in the primers) and inserted into the complementary sites of pGL3 basic luciferase vector (Promega). MDA-MD-231 cells (pretreated with scrambled siRNA, Twist siRNA, or PP2 (5 μM)) were transfected with 2 μg of pGL3-miR-10b promoter or pGL3 basic (Promega) constructs. All wells were additionally transfected with 1 μg of pCMV-β-gal as a transfection control. These cells were treated with or without HA (50 μg/ml) for 18 h, followed by incubating with reporter lysis buffer, and processed for luciferase or β-gal assays according to the manufacturer's protocols (Promega). Relative light units of 10b promoter samples were normalized to pGL3 basic and expressed as -fold increase in relative light units.

Immunofluorescence Staining Technique—MDA-MB-231 cells (untreated or pretreated with anti-CD44 antibody or a c-Src inhibitor, PP2 (5 μM)) were incubated with HA (50 μg/ml) or no HA for various time intervals (*e.g.* 0, 5 min, 10 min, 15 min, 30 min, or 24 h) at 37 °C, followed by fixing with 2% paraformaldehyde. Subsequently, these cells were rendered permeable by ethanol treatment, followed by incubation with Texas Red-labeled anti-Twist antibody followed by DAPI (a marker for nucleus). To detect nonspecific antibody binding, DAPI-labeled cells were incubated with Texas Red-conjugated normal IgG. No labeling was observed in control samples. In some cases, MDA-MB-231 cells (untreated or pretreated with anti-CD44 antibody or a c-Src inhibitor, PP2 (5 μM), or a ROK inhibitor, Y-27632 (5 μM), or transfected with Twist siRNA, scrambled siRNA, anti-miR-10b inhibitor, or miRNA-negative control) were treated with HA (50 μg/ml) (or no HA) for various time intervals (*e.g.* 0, 5 min, 10 min, 15 min, 30 min, or 24 h) at 37 °C were fixed with 2% paraformaldehyde. Subsequently, these cells were rendered permeable by ethanol treatment followed by incubation with FITC-conjugated phalloidin alone (to locate F-actin). These fluorescence-labeled samples were then examined with a confocal laser-scanning microscope.

ROK Activity Assay—MDA-MB-231 cells (untreated or pretreated with anti-CD44 antibody or a c-Src inhibitor, PP2 (5 μM), or a ROK inhibitor, Y-27632 (5 μM), or transfected with Twist siRNA, scrambled siRNA, anti-miR-10b inhibitor, or miRNA-negative control) were treated with HA (50 μg/ml) (or no HA) for various time intervals (*e.g.* 10 min, 30 min, 1 h, or 24 h) at 37 °C. These cells were then immediately lysed in Nonidet P-40 buffer (50 mM HEPES (pH 7.5), 150 mM NaCl, 20 mM $MgCl_2$, 1% Nonidet P-40, 1 mM Na_3VO_4, 1 mM NaF, Complete protease inhibitor mixture (Roche Applied Science), 1 mM PMSF, 1× Halt™ phosphatase inhibitor mixture (Pierce)) at 4 °C and centrifuged to obtain the lysates. Equal amounts of total lysates (~10 μg) or immunoprecipitation-purified ROK by preincubating lysates (~100 μg) with a rabbit anti-ROK antibody and agarose-conjugated anti-rabbit secondary antibody were assayed for Rho-kinase activity using a kit from CycLex (catalog no. CY-1160), following a protocol provided by the vendor. Basically, samples were incubated with a kinase reaction buffer with 0.1 mM ATP at 30 °C for 45 min in plates precoated with a Rho-kinase substrate corresponding to the C terminus of the recombinant myosin-binding subunit of myosin phosphatase (MBS), which contains a threonine residue that can be phosphorylated, and the product was detected by an HRP-conjugated antibody AF20 recognizing Thr^{696} of MBS as described previously (49). The HRP-mediated color reaction was then measured in a spectrophotometric plate reader at dual wavelengths of 450/540 nm. The absorbance data were analyzed. Controls included solvent control (no protein lysate) and inhibitor control (5 μM Y-27632 with protein lysate).

Tumor Cell Invasion Assay—Twenty-four transwell units were used for monitoring *in vitro* tumor cell invasion as described previously (29). Specifically, the 5-μm porosity polycarbonate filters coated with the reconstituted basement membrane substance Matrigel (Collaborative Research, Lexington, MA) were used for the cell invasion assay (29). MDA-MB-231 cells (1×10^4 cells/well) (untreated or pretreated with anti-CD44 antibody or a c-Src inhibitor, PP2 (5 μM), or a ROK inhibitor, Y-27632 (5 μM), or transfected with Twist siRNA, scrambled siRNA, anti-miR-10b inhibitor, or miRNA-negative control) were incubated with HA (50 μg/ml) for 18 h or no HA. The growth medium containing high glucose DMEM supplemented with 10% fetal bovine serum was placed in the lower chamber of the transwell unit. After an 18-h incubation at 37 °C in a humidified 95% air, 5% CO_2 atmosphere, cells on the upper side of the filter were removed by wiping with a cotton swab. Cell invasion processes were determined by measuring the cells that migrated (invaded) to the lower side of the polycarbonate filters by standard cell number counting methods as described previously (20). The CD44-specific cell invasion was determined by subtracting nonspecific cell invasion (*i.e.* cells that migrated (invaded) to the lower chamber in the presence of anti-CD44 antibody treatment). Each assay was performed in triplicate and repeated at least five times.

RESULTS

HA Profile in MDA-MB-231 Breast Tumor Cells

HA, one of the longest glycosaminoglycans, is composed of repeating disaccharide units of D-glucuronic acid-*N*-acetyl-D-glucosamine (50). It is often overexpressed at sites of breast tumor attachment (51) and is involved in CD44-mediated signaling and tumor progression (7–9). However, the profile of HA produced by breast tumor cells, such as MDA-MB-231 cells, has not been fully determined. In this study, we measured the HA profile of MDA-MB-231 cells by

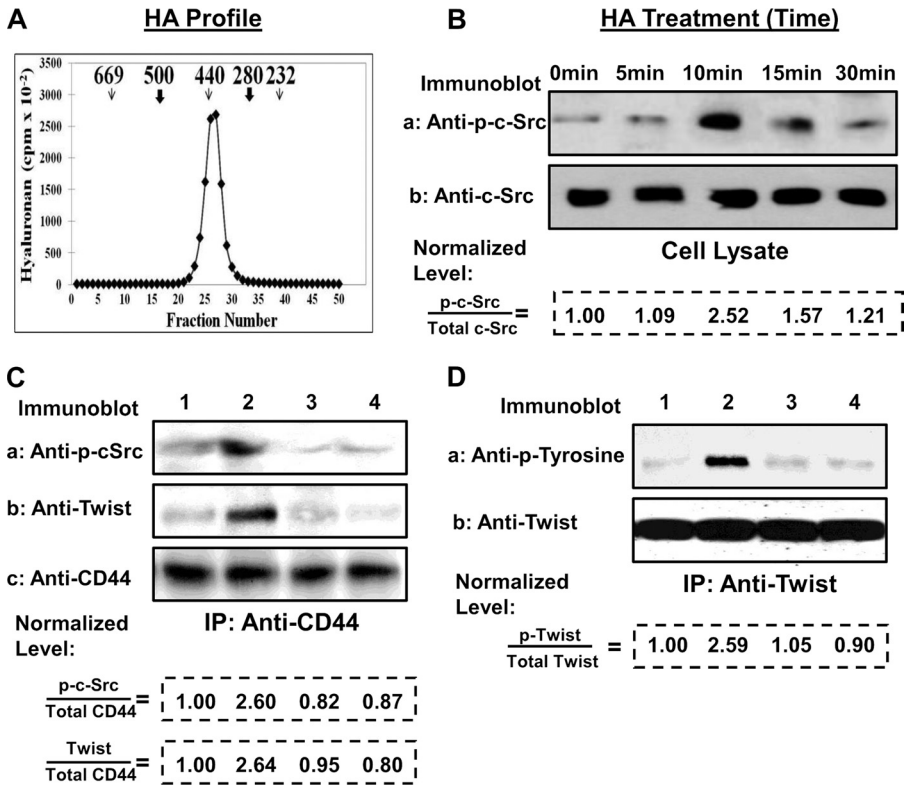

FIGURE 1. **Analyses of HA profile (*A*), HA-induced c-Src activation (*B*), and CD44 association with phosphorylated c-Src and Twist (*C* and *D*) in MDA-MB-231 cells.** *A*, HA profile analyses. MDA-MB-231 cells were metabolically labeled with [^{3}H]glucosamine. HA was then collected from the medium and analyzed by Hiprep^{TM} Sephacryl^{TM} 400 HR (*S-400HR*) gel filtration as described under "Materials and Methods." (Markers used in the Sephacryl^{TM} 400 HR column chromatography include two HA markers (500 and 280 kDa; indicated by *arrowheads*) and three protein markers (232, 440, and 669 kDa; indicated by *arrows*).) *B*, HA-induced c-Src kinase activation. Cell lysates were prepared from MDA-MB-231 cells treated with HA (50 μg/ml) for various time intervals (*e.g.* 0, 5, 10, 15, and 30 min) followed by immunoblotting with anti-phospho-Src (pY^{418}) antibody or anti-c-Src antibody (as a loading control). (The ratio of phosphorylated c-Src (*a*) and total c-Src (the loading control) (*b*) was determined by densitometry, and the levels were normalized to untreated (0 min of HA treatment) cell value (designated as 1.00); the values expressed represent an average of triplicate determinations of three experiments with an S.D. value of <5%.) *C*, HA-induced CD44 signaling complex formation in MDA-MB-231 cells. Cells were first solubilized with 1% Nonidet P-40 (Nonidet P-40) buffer followed by immunoprecipitation (*IP*) and/or immunblot by anti-CD44 antibody or anti-phospho-c-Src antibody or anti-Twist antibody, respectively, as described under "Materials and Methods." Phosphorylated c-Src and Twist in the CD44 complex were detected by anti-CD44-immunoprecipitation, followed by immunoblotting with anti-phospho-c-Src antibody (*a*) or anti-Twist antibody (*b*) or reblotting with anti-CD44 (*c*) as a loading control using MDA-MB-231 cells treated with no HA (*lane 1*) or with HA (50 μg/ml) for 10 min (*lane 2*) or pretreated with anti-CD44 antibody (*lane 3*) or PP2 (*lane 4*) for 1 h followed by 10 min of HA (50 μg/ml) addition. (The ratio of phosphorylated c-Src (*a*) and total CD44 (the loading control) (*c*) and the ratio of Twist (*b*) and total CD44 (the loading control) (*c*) were determined by densitometry, and the levels were normalized to untreated (no HA treatment) cell value (*lane 1*; designated as 1.00); the values expressed represent an average of triplicate determinations of four experiments with an S.D. value of <5%.) *D*, phosphorylation of Twist was analyzed by solubilizing MDA-MB-231 cells with 1% Nonidet P-40 (Nonidet P-40) buffer, followed by immunoprecipitation with anti-Twist antibody followed by immunoblotting with anti-phosphotyrosine antibody (*a*) or anti-Twist antibody (as a loading control) (*b*) using cell lysates obtained from MDA-MB-231 cells treated with no HA (*lane 1*) or with HA for 10 min (*lane 2*) or pretreated with anti-CD44 antibody (*lane 3*) or PP2 (*lane 4*) followed by 10 min of HA addition. (The ratio of phosphorylated Twist (*a*) and total Twist (the loading control) (*b*) was determined by densitometry, and the levels were normalized to untreated (no HA treatment) cell value (*lane 1*; designated as 1.00); the values expressed represent an average of triplicate determinations of four experiments with an S.D. value of <5%.

metabolically labeling these cells with [^{3}H]glucosamine for 18 h. Hyaluronan was then recovered from the medium (also the cells) and analyzed using Sephacryl S-400 gel filtration methods according to the procedures described previously (50). The large majority of the HA has a molecular mass of ~400 kDa and is accumulated in the medium (Fig. 1*A*). Very little HA is associated with the MDA-MB-231 cells (data not shown). The question of whether this HA (molecular mass ~400 kDa) plays a significant role in regulating oncogenic signaling is addressed in this study.

HA/CD44-mediated c-Src Activation and Twist Phosphorylation/Signaling in MDA-MB-231 Breast Tumor Cells

The full catalytic activity of c-Src kinase requires phosphorylation of tyrosine 418 (52). Previous studies have shown that HA-CD44 interaction promotes c-Src phosphorylation at the tyrosine 418 residue and its activation in certain epithelial tumor cells (15). Using specific anti-phospho-Src antibody (anti-Src-(Tyr(P)^{418}); designed to detect the activated form of c-Src kinase), we found that the highest level of c-Src activation in MDA-MB-231 cells occurred at 10 min following HA addition (Fig. 1*B*, *lane 3*). A relatively lower level of c-Src kinase activation was detected when MDA-MB-231 cells were treated with HA for either 5, 15, or 30 min or with no HA (Fig. 1*B*). Therefore, the 10-min HA treatment was used to monitor HA-mediated c-Src signaling events as described below.

In order to investigate whether there is a direct interaction between CD44 and phosphorylated c-Src in breast tumor cells, we performed anti-CD44-mediated immunoprecipitation followed by anti-phospho-c-Src (*Anti-p-c-Src*) immunoblot (Fig. 1*C*, *a*, *lane 1*) or anti-CD44 immunoblot (Fig. 1*C*, *b*, *lane 1*) using untreated MDA-MB-231 cells. Our results indicate that a very low level of phosphorylated c-Src (Fig. 1*C*, *a*, *lane 1*) is present in the anti-CD44-immunoprecipitated materials (Fig. 1*C*, *b*, *lane 1*). Subsequently, we determined that a 10-min HA treatment induced the recruitment of a significant amount of phosphorylated c-Src (Fig. 1*C*, *a*, *lane 2*) into the CD44-c-Src complex (Fig. 1*C*, *c*, *lane 2*). Pretreatment of MDA-MB-231 cells with anti-CD44 antibody or a c-Src inhibitor, PP2, followed by a 10-min HA treatment resulted in a significant reduction of phosphorylated c-Src (Fig. 1*C*, *a*, *lanes 3* and *4*) in the anti-CD44-immunoprecipitated materials (Fig. 1*C*, *c*, *lanes 3* and *4*). These findings establish the fact that phosphorylated c-Src (possibly active forms of c-Src) is accumulated in a complex with

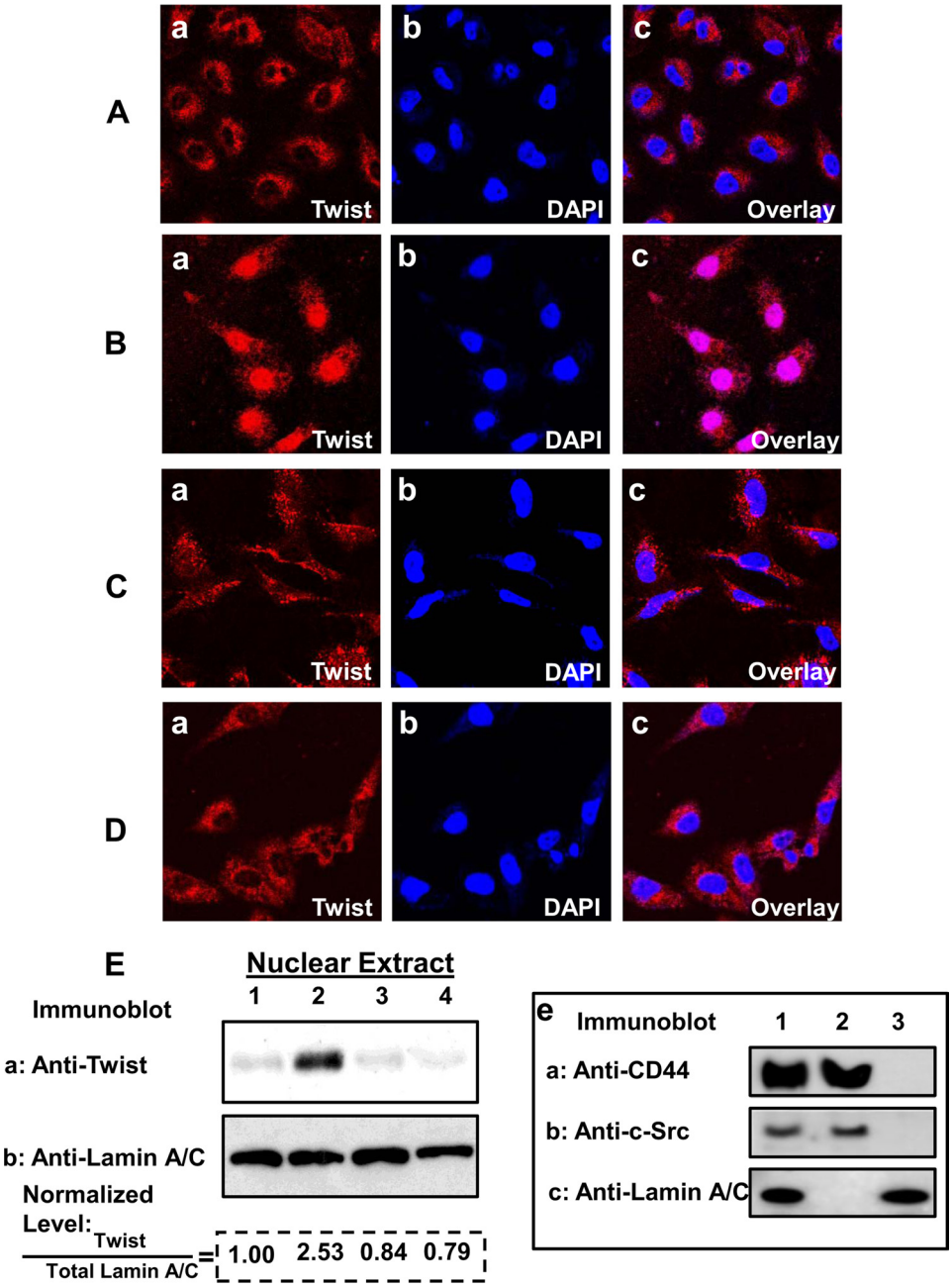

FIGURE 2. **Immunocytochemical and biochemical analyses of HA/CD44-induced Twist nuclear translocation in MDA-MB-231 cells.** *A–D*, immunostaining of Twist. MDA-MB-231 cells (untreated or pretreated with anti-CD44 antibody or PP2 followed by HA addition for 15 min or no HA addition) were fixed by 2% paraformaldehyde. Subsequently, cells were rendered permeable by ethanol treatment and immunostained with Twist and DAPI (a nuclear marker) (*A–D*) as described under "Materials and Methods." *A*, Texas Red-labeled anti-Twist (*red*) (*a*), DAPI (*blue*) (*b*), and an *overlay image* (*c*) of *a* and *b* in cells without HA treatment. *B*, Texas Red-labeled anti-Twist (*red*) (*a*), DAPI (*blue*) (*b*) and an *overlay image* (*c*) of *a* and *b* in cells with 15 min of HA treatment. *C*, Texas Red-labeled anti-Twist (*red*) (*a*), DAPI (*blue*) (*b*), and an *overlay image* (*c*) of *a* and *b* in cells pretreated with anti-CD44 antibody for 1 h followed by 15 min of HA addition. *D*, Texas Red-labeled anti-Twist (*red*) (*a*), DAPI (*blue*) (*b*), and an *overlay image* (*c*) of *a* and *b* in cells pretreated with PP2 for 1 h followed by 15 min of HA addition. *E*, analyses of HA/CD44-induced Twist localization in the nuclear fraction. MDA-MB-231 cells (untreated or pretreated with anti-CD44 antibody or PP2 for 1 h) were incubated with HA (50 μg/ml) (or without HA) for 15 min at 37 °C. Nuclear fractions of these cells were then prepared followed by immunoblotting with anti-Twist antibody (*a*) or anti-lamin A/C antibody (as a loading control) (*b*) as described under "Materials and Methods" (*lane 1*, untreated cells; *lane 2*, cells treated with HA for 15 min; *lane 3*, cells pretreated with anti-CD44 antibody for 1 h plus 15 min of HA addition; *lane 4*, cells pretreated with PP2 for 1 h plus 15 min of HA addition). (The ratio of Twist (*a*) and total lamin A/C (the loading control) (*b*) in the nuclear extract was determined by densitometry, and the levels were normalized to untreated (no HA treatment) cell value (*lane 1*; designated as 1.00); the values expressed represent an average of triplicate determinations of four experiments with an S.D. value of $<5\%$.) *e*, immunoblot analyses of various cellular fractions, including total cell lysate (*lane 1*), cytosolic fraction (*lane 2*), and nuclear extract (*lane 3*) using specific antibodies against plasma membrane protein, CD44 (*a*), the cytosolic protein, c-Src (*b*), and nuclear marker protein, lamin A/C (*c*), respectively.

CD44 (in whole cells) following HA treatment of the MDA-MB-231 breast tumor cells.

Twist can be activated by c-Src in CD44-expressing breast tumor cells (42). In order to investigate whether there is any signaling interaction between CD44-linked c-Src and Twist, we performed anti-CD44 immunoprecipitation followed by anti-c-Src and anti-Twist antibody-mediated immunoblot as shown in Fig. 1. Our results indicate that CD44-linked phospho-c-Src (isolated from MDA-MB-231 cells treated with HA) is capable of recruiting the transcription factor, Twist (Fig. 1*C*, *b*, *lane 2*) into CD44-associated multimolecular complexes (Fig. 1*C*, *c*, *lane 2*). Further analysis indicates that significant Twist phosphorylation occurs in MDA-MB-231 cells treated with HA for 10 min (Fig. 1*D*, *a* and *b*, *lane 2*). Specifically, Twist phosphorylation was identified with anti-Twist antibody followed by anti-phosphotyrosine antibody immunoblot. Because phosphorylated Twist has a molecular mass of ~22 kDa (clearly different from phosphorylated c-Src (~56 kDa)), we conclude that Twist phosphorylation occurs in cells following HA treatment. In contrast, Twist phosphorylation was relatively low in MDA-MB-231 cells without any HA treatment (Fig. 1*D*, *a* and *b*, *lane 1*) or MDA-MB-231 cells pretreated with anti-CD44 antibody or PP2 (a c-Src inhibitor) followed by HA treatment (Fig. 1*D*, *a* and *b*, *lanes 3* and *4*). Thus, HA-activated Twist phosphorylation is both CD44-specific and c-Src-dependent.

In addition, we found that Twist could be translocated from the cytosol to the nucleus after HA treatment (Fig. 2, *B* (*a–c*) and E (*a* and *b*, *lane 2*)), and the maximal level of Twist nuclear translocation in MDA-MB-231 cells could be detected at 15 min following HA addition (Table 1). In contrast, the majority of Twist was distributed in the cytosol, and only a low level of Twist was present in the nucleus of MDA-MB-231 cells, either pretreated with anti-CD44 antibody

TABLE 1

HA-mediated Twist nuclear translocation and cytoskeleton reorganization in MDA-MB-231 cells

Shown are the effects of HA on Twist nuclear translocation (top) and cytoskeleton reorganization (bottom). The number of cells displaying both Twist nuclear localization (top) and F-actin assembly (bottom) was counted under the microscope. Specifically, every cell in the field was examined for the occurrence of the cell phenotypes (*e.g.* with or without Twist nuclear localization and F-actin formation). At least 200–300 cells (in 12 different fields) were examined in each sample. Quantitative values describing the percentage of cells displaying Twist nuclear localization and F-actin reorganization in each sample were expressed as percentage of control. Untreated cells in control are designated as 100%. The values expressed represent an average of triplicate determinations of five experiments with an S.D. value less than ±5%.

Treatments	Twist nuclear translocation[a] (percentage of control)
	%
No treatment (control)	100 ± 5
HA treatment for 10 min	110 ± 8
HA treatment for 15 min	280 ± 14
HA treatment for 30 min	155 ± 5
HA treatment for 24 h	123 ± 7
Treatments	**F-actin assembly[b] (percentage of control)**
	%
No treatment (control)	100 ± 4
HA treatment for 10 min	110 ± 6
HA treatment for 15 min	156 ± 9
HA treatment for 30 min	263 ± 10
HA treatment for 24 h	225 ± 15

[a] MDA-MB-231 cells were treated with HA (50 μg/ml) or no HA for various time intervals (e.g., 0, 10 min, 15 min, 30 min, or 24 h) at 37 °C and fixed with 2% paraformaldehyde. Subsequently, these cells were rendered permeable by ethanol treatment followed by incubation with Texas Red-labeled anti-Twist antibody followed by DAPI (a marker for nucleus). To detect nonspecific antibody binding, DAPI-labeled cells were incubated with Texas Red-conjugated normal IgG. No labeling was observed in control samples, as described under "Materials and Methods."

[b] MDA-MB-231 cells were treated with HA (50 μg/ml) or no HA for various time intervals (*e.g.* 0, 10 min, 15 min, 30 min, or 24 h) at 37 °C and fixed with 2% paraformaldehyde. Subsequently, these cells were rendered permeable by ethanol treatment followed by incubation with FITC-conjugated phalloidin alone (to locate F-actin). These fluorescence-labeled samples were then examined with a confocal laser-scanning microscope, as described under "Materials and Methods."

plus HA (Fig. 2, *C* (*a*–*c*) and *E* (*a* and *b*, *lane 3*)) or without any HA treatment (Fig. 2*A* (*a*–*c*) and *E* (*a* and *b*, *lane 1*)). Down-regulation of c-Src activity by treating MDA-MB-231 cells with PP2 (a c-Src inhibitor) significantly inhibited HA/CD44-mediated Twist nuclear translocation (Fig. 2, *D* (*a*–*c*) and *E* (*a* and *b*, *lane 4*)). In order to verify the purity of the nuclear fraction (Fig. 2*e*, *lane 3*), we performed immunoblot analyses of various cellular fractions (*e.g.* nuclear extract, cytosolic fraction, and total cell lysate) using specific antibodies against nuclear marker protein, lamin A/C, plasma membrane protein, CD44 and the cytosolic protein, c-Src (Fig. 2*e*, *lanes 1–3*). Our data indicate that lamin A/C appears to be the predominant protein associated with the nuclear fraction (Fig. 2*e*, *lane 3*). Very little plasma membrane protein (*e.g.* CD44) or cytosolic protein (*e.g.* c-Src) was detected in the nuclear fraction (Fig. 2*e*, *lane 3*). Therefore, we conclude that the amount of cytosolic protein contamination in our nuclear fraction is minimal. Thus, our observations strongly support the contention that nuclear translocation of Twist occurs in MDA-MB-231 cells after HA/CD44-mediated Src activation.

Role of Twist in Regulating miR-10b Expression in HA/CD44 and c-Src-activated MDA-MB-231 Cells

Binding of Twist to E-box Elements in the miR-10b Promoter in Breast Tumor Cells—Several predicted E-box elements are located upstream of miR-10b (38), a class of miRNA known to

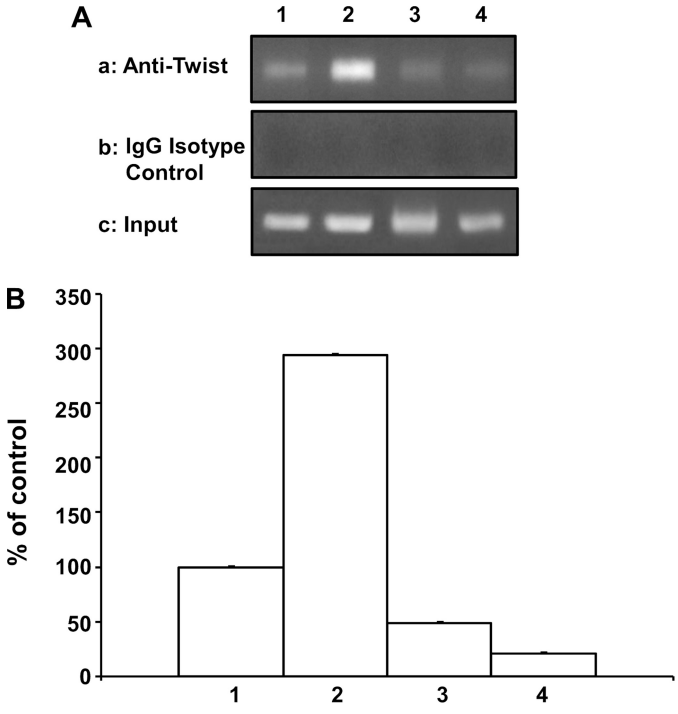

FIGURE 3. **Interaction between Twist and the miR-10b promoter in MDA-MB-231 cells.** *A*, *in vivo* binding of Twist to the miR-10b promoter in breast tumor cells. A ChIP assay was performed in MDA-MB-231 cells following the protocols described under "Materials and Methods" using the E-box-containing miR-10b promoter-specific primers by PCR. Identical volumes from the final precipitate were used for the PCRs (*lane 1*, untreated cells; *lane 2*, cells treated with HA for 30 min; *lane 3*, cells pretreated with anti-CD44 antibody for 1 h plus 30 min of HA addition; *lane 4*, cells pretreated with PP2 for 1 h plus 30 min of HA addition) (*a*, anti-Twist-mediated immunoprecipitate; *b*, IgG isotype control-mediated immunoprecipitate; *c*, total input immunoprecipitate). *B*, measurement of miR-10b transcriptional activation. MDA-MB-231 cells (transfected with scrambled siRNA followed by 24 h of HA incubation (*bar 2*) or no HA addition (*bar 1*) or Twist siRNA plus 24 h of HA incubation (*bar 3*) or pretreated with PP2 for 1 h followed by 24 h of HA incubation (*bar 4*)) were co-transfected with miR-10b promoter-Luc (luciferase reporter vector) and a plasmid encoding β-galactosidase (to enable normalization for transfection efficiency). After 24 h, expression of the reporter (luciferase) and the control (β-galactosidase) genes were determined using enzyme assays and luminometry as described under "Materials and Methods." The activity of miR-10b-specific transcriptional activation in untreated cells is designated as 100% (control). The values expressed in this figure represent an average of triplicate determinations of five experiments with an S.D. value of <5%.

be associated with breast tumor invasion and metastasis. To examine whether Twist directly interacts with the E-box elements in the promoter region of miR-10b, anti-Twist antibody-specific ChIP assays were performed in MDA-MB-231 cells. As shown in Fig. 3*A*, the PCR from anti-Twist-mediated precipitations (from HA-treated MDA-MB-231 cells) resulted in a specific amplification product using a primer pair specific for the miR-10b promoter region containing the E-boxes (Fig. 3*A*, *a*, *lane 2*). In contrast, there was very little Twist binding to the miR-10b upstream promoter region in cells pretreated with anti-CD44 antibody (Fig. 3*A*, *a*, *lane 3*) or PP2 (a c-Src kinase inhibitor) (Fig. 3*A*, *a*, *lane 4*) followed by HA addition or without HA treatment (Fig. 3*A*, *a*, *lane 1*). Identical amplification products were detected in the positive controls from total input chromatin (Fig. 3*A*, *c*, *lanes 1–4*). Moreover, no amplification was seen in samples that were processed in IgG isotype control-mediated precipitation (Fig. 3*A*, *b*, *lanes 1–4*). We observed similar results by quantitative RT-PCR (data not shown). Thus,

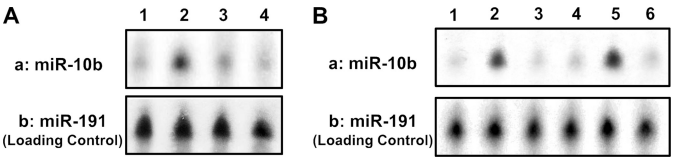

FIGURE 4. **Detection of HA/CD44-induced miR-10b production in MDA-MB-231 cells.** Detection of miR-10b in MDA-MB-231 cells using RNase protection assay as described under "Materials and Methods." *A*, autoradiogram of miR-10b (*a*) detected in MDA-MB-231 cells treated with no HA (*lane 1*) or with HA for 2 h (*lane 2*) or pretreated with anti-CD44 antibody (*lane 3*) or PP2 (*lane 4*) for 1 h followed by HA addition for 2 h; *B*, autoradiogram of miR-10b detected in MDA-MB-231 cells incubated with scrambled sequence siRNA (without HA (*lane 1*) or with 2 h of HA treatment (*lane 2*)) or incubated with Twist siRNA plus 2 h of HA treatment (*lane 3*) or incubated with miRNA-negative control (without HA (*lane 4*) or with 2 h of HA treatment (*lane 5*)) or incubated with an anti-miR-10b inhibitor plus 2 h of HA treatment (*lane 6*). (The autoradiogram of miR-191 (*b*) in each gel lane was used as a loading control.)

these results verify that Twist binds directly (or forms as part of the complex) to the promoter region of miR-10b in MDA-MB-231 cells following HA-CD44 interaction.

Involvement of Twist in Regulating miR-10b Transcription in Breast Tumor Cells—To further demonstrate the involvement of Twist in regulating the transcription of miR-10b, MDA-MB-231 cells were transfected with an E-box-containing a miR-10b promoter-luciferase construct and a plasmid encoding β-galactosidase to monitor normalization of the transfection efficiency. Our results indicate that transcriptional activity of miR-10b is greatly stimulated in MDA-MB-231 cells treated with scrambled siRNA plus HA (Fig. 3*B*, *bar 2*) as compared with those cells treated with no HA (Fig. 3*B*, *bar 1*). The fact that pretreatment of cells with Twist siRNA (Fig. 3*B*, *bar 3*) or with PP2 (a c-Src inhibitor) (Fig. 3*B*, *bar 4*) followed by HA addition significantly reduced the transcriptional activity of miR-10b verifies that Twist signaling and c-Src activation can transcriptionally activate miR-10b promoter activity in HA-treated breast tumor cells.

Production of miR-10b in Breast Tumor Cells—To determine whether miR-10b levels are increased following the binding of HA to CD44, we first prepared small RNAs followed by an RNase protection assay using the miRNA Detection Kit (Ambion). Our results indicate that an elevated level of miR-10b expression was detected in MDA-MD-231 cells following a 2-h incubation with HA (Fig. 4*A*, *a*, *lane 2*) as compared with cells not treated with HA (Fig. 4*A*, *a*, *lane 1*). The increase in expression of miR-10b was specifically a result of the interaction between HA and CD44 because pretreatment of MDA-MB-231 cells with anti-CD44 antibody plus HA addition significantly reduced miR-10b production (Fig. 4*A*, *a*, *lane 3*). When the c-Src inhibitor PP2 was added to these breast tumor cells, the expression of miR-10b in HA-treated cells appeared to be significantly decreased (Fig. 4*A*, *a*, lane 4), indicating that c-Src is involved in HA-mediated production of miR-10b. Our results also show that the level of miR-10b is increased in MDA-MB-231 cells treated with scrambled sequence siRNA plus HA compared with those cells without HA treatment (Fig. 4*B*, *a*, *lane 1 versus lane 2*). MDA-MB-231 cells treated with Twist siRNA show significantly less HA-induced miR-10b expression (Fig. 4*B*, *a*, *lane 3*). Moreover, we found that the expression of miR-10b could be induced in cells treated with an miRNA-negative control upon the addition of HA (Fig. 4*B*, *a*, *lane 5 versus lane 4*). In contrast, the treatment of MDA-MB-231 cells with an anti-miR-10b inhibitor plus HA resulted in a decrease in miR-10b expression (Fig. 4*B*, *a*, *lane 6 versus lane 5*). We believe that these changes in miR-10b expression under various treatment conditions were not due to the variations of RNA extracted from each sample because there were very similar levels of the miR-191 control in all samples (Fig. 4, *A* (*b*, *lanes 1–4*) and *B* (*b*, *lanes 1–6*)). Taken together, our findings strongly suggest that HA/CD44-activated Twist and c-Src signaling plays an important role in the production of miR-10b in breast tumor cells.

Effects of HA/CD44-activated miR-10b on HOXD10 Expression, RhoGTPase Up-regulation, ROK-mediated Cytoskeleton Function, and Breast Tumor Cell Invasion

Previous studies indicate that miR-10b may function as an oncogene and play a role in promoting tumor cell migration and invasion, in part through down-regulation of several tumor suppressor genes/proteins, including HOXD10, and up-regulation of RhoGTPases (38). However, the identification of miR-10b-specific downstream target(s) and oncogenic event(s) that contribute to HA/CD44-dependent breast tumor cell invasion has not been established.

HOXD10 and RhoGTPases as the Possible Downstream Target(s) for miR-10b in Breast Tumor Cells—The homeobox transcription factor, HOXD10, has been identified as one of the tumor suppressor genes regulated by miR-10b (70). It promotes or maintains a differentiation phenotype in epithelial cells (38). In this study, we found that a basal level of HOXD10 expression was present in cells with no HA treatment (Fig. 5, *A* and *B* (*a* and *b*, *lane 1*)). Down-regulation of HOXD10 appeared to occur as early as 30–60 min after HA treatment (Fig. 5*A*). However, 24-h HA treatment significantly reduced the expression of tumor suppressor protein HOXD10 in MDA-MB-231 cells (Fig. 5*B*, *a* and *b*, *lane 2*). In contrast, in cells pretreated with anti-CD44 antibody or PP2 (a c-Src inhibitor), HA treatment failed to decrease HOXD10 expression (Fig. 5*B*, *a* and *b*, *lanes 3* and *4*). Thus, the reduction of HOXD10 expression appears to be HA-dependent and CD44/c-Src-specific in breast tumor cells. We also confirmed that down-regulation of miR-10b by treating MDA-MB-231 cells with an anti-miR-10b inhibitor (but not a negative control miRNA) promoted up-regulation of HOXD10 expression in the presence of HA (Fig. 5*B* (*a*, *lane 10 versus lanes 8* and *9*)). These results support the contention that miR-10b (mediated by HA-CD44 binding) is acting as an oncogene by down-regulating the expression of the tumor suppressor, HOXD10. It is also noted that a basal level of HOXD10 expression was detected in cells treated with scrambled sequence siRNA without HA addition (Fig. 5*B*, *a*, *lane 5*). In contrast, significant reduction of HOXD10 expression was observed in cells treated with HA (Fig. 5*B*, *a*, *lane 6*). Furthermore, treatment of MDA-MB-231 cells with Twist siRNA (in the presence of HA) displayed an elevated level of HOXD10 expression (Fig. 5*B*, *a*, *lane 7 versus lane 6*). These findings indicate that the signaling network consisting of c-Src, Twist, and miR-10b is functionally coupled with the inhibition of the tumor suppressor protein (HOXD10) expression. These spe-

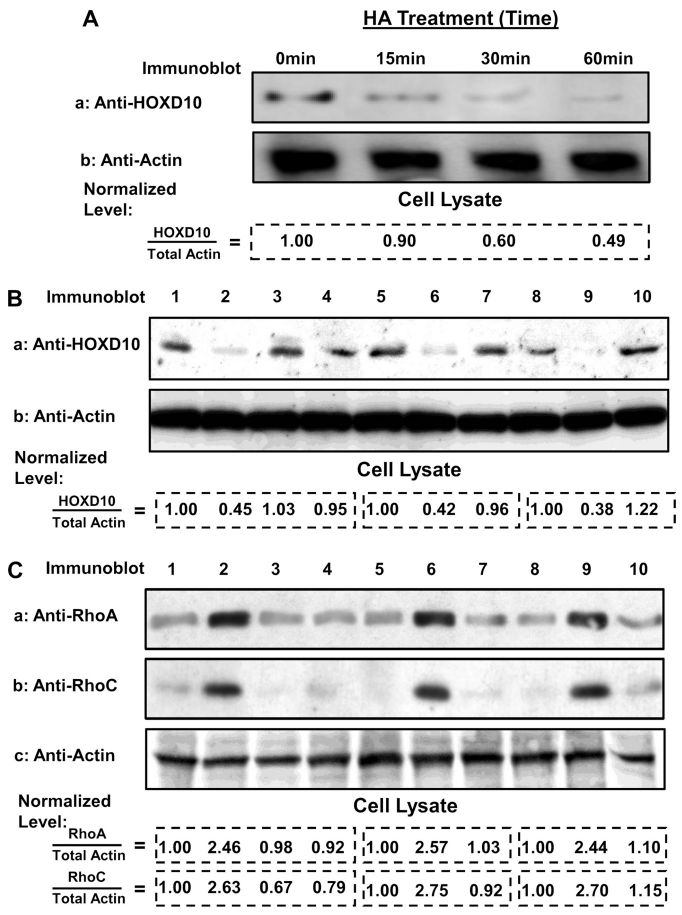

FIGURE 5. **Analyses of HA/CD44-mediated HOXD10 and RhoGTPase expression in MDA-MB-231 cells.** Detection of HA/CD44-induced HOXD10 and RhoGTPase (RhoA/RhoC) expression in MDA-MB-231 cells was performed by solubilizing cells with 1% Nonidet P-40 (Nonidet P-40) buffer followed by immunoblotting with anti-HOXD10 antibody or anti-RhoA antibody or anti-RhoC antibody, respectively as described under "Materials and Methods." *A*, HA-induced HOXD10 expression. Cell lysates were prepared from MDA-MB-231 cells treated with HA (50 μg/ml) for various intervals of time (*e.g.* 0, 15, 30, and 60 min) followed by immunoblotting with anti-HOXD10 antibody or anti-actin antibody (as a loading control). (The ratio of HOXD10 (*a*) and total actin (the loading control) (*b*) was determined by densitometry, and the levels were normalized to untreated (0 min of HA treatment) cell value (designated as 1.00); the values expressed represent an average of triplicate determinations of three experiments with an S.D. of <5%.) *B*, detection of the expression of HOXD10 by anti-HOXD10-mediated immunoblotting (*a*) using cell lysate isolated from MDA-MB-231 cells treated with no HA (*lane 1*) or with HA for 24 h (*lane 2*) or pretreated with anti-CD44 antibody (*lane 3*) or PP2 (*lane 4*) for 1 h followed by 24 h of HA addition or treated with scrambled sequence siRNA (without HA (*lane 5*) or with HA for 24 h (*lane 6*)) or treated with Twist siRNA plus HA for 24 h (*lane 7*) or treated with miRNA-negative control (without HA (*lane 8*) or with HA for 24 h (*lane 9*)) or treated with anti-miR-10b inhibitor plus HA for 24 h (*lane 10*). The amount of actin detected by anti-actin-mediated immunoblot (*b*) in each gel lane was used as a loading control. (The ratio of HOXD10 (*a*) and total actin (the loading control) (*b*) was determined by densitometry, and the levels were normalized to the untreated (no HA treatment) cell value (*lane 1*; designated as 1.00) for *lanes 2–4*, normalized to the scrambled sequence siRNA-treated cell value (*lane 5*; designated as 1.00) for *lanes 6* and *7*, or normalized to the miRNA-negative control cell value (*lane* 8; designated as 1.00) for *lanes 9* and *10*. The values expressed represent an average of triplicate determinations of four experiments with an S.D. value of <5%.) *C*, detection of the expression of RhoA or RhoC by anti-RhoA or anti-RhoC-mediated immunoblotting (*a* and *b*) using cell lysate isolated from MDA-MB-231 cells treated with no HA (*lane 1*) or with HA for 24 h (*lane 2*) or pretreated with anti-CD44 antibody (*lane 3*) or PP2 (*lane 4*) for 1 h followed by 24 h of HA addition or treated with scrambled sequence siRNA (without HA (*lane 5*) or with HA for 24 h (*lane 6*)) or treated with Twist siRNA plus HA for 24 h (*lane 7*) or treated with miRNA-negative control (without HA (*lane 8*) or with HA for 24 h (*lane 9*)) or treated with anti-miR-10b inhibitor plus HA for 24 h (*lane 10*). The amount of actin detected by anti-actin-mediated immunoblot (*c*) in each gel lane was used as a loading control. (The ratio of RhoA (*a*) and total actin (the loading control) (*c*) or the ratio of RhoC (*b*) and total actin (the loading control) (*c*) was determined by densitometry, and the levels were normalized to untreated (no HA treatment) cell value (*lane 1*; designated as 1.00) for *lanes 2–4* or normalized to scrambled sequence siRNA-treated cell value (*lane 5*; designated as 1.00) for *lanes 6* and *7* or normalized to miRNA-negative control cell value (*lane 8*; designated as 1.00) for *lanes 9* and *10*. The values expressed represent an average of triplicate determinations of four experiments with an S.D. value of <5%.)

cific effects may facilitate the progression of HA/CD44-activated breast tumor cells.

To determine how these changes in the tumor suppressor protein (HOXD10) expression and function by miR-10b (via HA/CD44 interaction and c-Src/Twist signaling) may affect breast tumor cell-specific behaviors (*e.g.* RhoGTPases, cytoskeleton function, and breast tumor invasion), we analyzed the expression of two RhoGTPases, RhoA and RhoC. First, immunoblot analyses using a panel of antibodies (*e.g.* RhoA antibody and anti-RhoC antibody) were employed to detect the production of the two proteins, RhoA and RhoC, in MDA-MB-231 cells. Our data indicate that the expressions of both RhoA and RhoC were significantly increased in MDA-MB-231 cells treated with HA (Fig. 5*C*, *a* and *b*, *lane 2 versus lane 1*). In contrast, these two proteins (*e.g.* RhoA and RhoC) were present in relatively low amounts in MDA-MB-231 cells not treated with HA (Fig. 5*C*, *a* and *b*, *lane 1 versus lane 2*) or in those cells pretreated with anti-CD44 antibody or PP2 (a c-Src inhibitor) followed by HA addition (Fig. 5*C*, *a* and *b*, *lane 3* and *lane 4 versus lane 2*). These findings support the notion that the expression of RhoA and RhoC is both HA- and CD44-dependent. Most importantly, down-regulation of miR-10b by treating cells with an anti-miR-10b inhibitor significantly attenuated the HA/CD44-activated expression of RhoA and RhoC (Fig. 5*C*, *a* and *b*, *lane 10 versus lane 9* and *lane 8*). In contrast, MDA-MB-231 cells treated with an miRNA-negative control were capable of inducing the expression of both RhoA and RhoC in the presence of HA (Fig. 5*C*, *a* and *b*, *lane 8 versus lane* 9). Furthermore, we observed that the expression of RhoA and RhoC were significantly inhibited when MDA-MB-231 cells were pretreated with Twist siRNA (Fig. 5*C*, *a* and *b*, *lane 7 versus lane 6*) but not scrambled sequence siRNA followed by HA addition (Fig. 5*C*, *a* and *b*, *lane 5 versus lane 6*), respectively. The fact that down-regulation of both c-Src/Twist signaling and miR-10b production inhibits the expression of RhoA and RhoC indicates that the HA/CD44-activated c-Src/Twist signaling and miR-10b function actively participate in the up-regulation of RhoGTPases, such as RhoA and RhoC, in breast tumor cells.

Effect of miR-10b on RhoGTPase-activated ROK, F-actin Reorganization, and Breast Tumor Cell Invasion—Several enzymes have been identified as possible downstream targets for RhoA and RhoC in regulating cytoskeleton-mediated biological events. One such enzyme is ROK (30, 31). To further assess whether ROK might be regulated by the HA-CD44 interaction with c-Src/Twist signaling and miR-10b production, we performed a ROK activity assay in the presence or absence of HA or anti-CD44 antibody plus HA. In the absence of HA, MDA-MB-231 cells displayed a low level of ROK activity (Table

TABLE 2

Measurement of HA-mediated ROK activity

Shown are the effects of various agents on HA-induced ROK activity (top), the effects of Twist siRNA on HA-mediated ROK activity (middle), and the effects of anti-miR-10b inhibitor on HA-mediated ROK activity (bottom). All data represent mean ± S.E. (with $n = 5$) of the ROK activity detected in each sample.

Treatments	Relative kinase activity (percentage of control)[a]
	%
No treatment (control)	100 ± 5
HA treatment	250 ± 13
HA + anti-CD44 antibody treatment	102 ± 4
HA + PP2 treatment	113 ± 5
HA + Y27632 treatment	92 ± 3

Treatments	Relative kinase activity (percentage of control)	
	Scrambled siRNA-treated cells	Twist siRNA-treated cells
	%	%
No treatment (control)	100 ± 4	98 ± 3
HA treatment	242 ± 15	102 ± 5

Treatments	Relative kinase activity (percentage of control)	
	miRNA negative control-treated cells	Anti-miR-10b inhibitor-treated cells
	%	%
No treatment (control)	100 ± 5	103 ± 5
HA treatment	248 ± 10	105 ± 4

[a] *In vitro* ROK activity in MDA-MB-231 cells (untreated or pretreated with anti-CD44 antibody or PP2 (5 μM) or Y27632 (5 μM) or transfected with Twist siRNA or scrambled siRNA or miRNA negative control or anti-miR-10b inhibitor followed by 50 μg/ml HA addition) was measured as described under "Materials and Methods." Specifically, samples were incubated with a kinase reaction buffer with ATP in plates precoated with a Rho-kinase substrate corresponding to the C terminus of recombinant MBS, which contains a threonine residue that can be phosphorylated, and the product was then detected by an HRP-conjugated antibody AF20 recognizing Thr^{696} of MBS. An HRP-mediated color reaction was then measured in a spectrophotometric plate reader at dual wavelengths of 450/540 nm. The absorbance data were analyzed. The ROK activity in untreated cells (top; control), scrambled siRNA-treated cells without HA (middle; control), or miRNA negative control-treated cells without HA (bottom; control) is designated as 100%. The values expressed in this table represent an average of triplicate determinations of five experiments.

2, top). However, the addition of HA greatly enhanced ROK activity (Table 2, top). Furthermore, pretreatment of these tumor cells with anti-CD44 antibody or a ROK inhibitor, Y27632, followed by HA addition significantly decreases HA-mediated ROK activity (Table 2, top). This result indicates that HA-CD44 interaction promotes ROK activation in breast tumor cells. Moreover, down-regulation of c-Src or Twist or miR-10b (by treating tumor cells with PP2 (a c-Src inhibitor) (Table 2, top) or transfecting tumor cells with Twist siRNA or anti-miR-21 inhibitor (but not scrambled sequence siRNA or an miRNA-negative control) (Table 2, middle and bottom)) effectively attenuates HA-mediated ROK activity in MDA-MB-231 cells. Together, these findings indicate that the HA/CD44-mediated c-Src-Twist signaling pathways and miR-10b function play an important role in ROK activation in breast cancer cells.

To further analyze whether the ROK downstream effectors (*e.g.* actin-cytoskeleton reorganization and breast tumor cell invasion) might be regulated by the HA-CD44 interaction with c-Src/Twist signaling and miR-10b production, we performed both immunolocalization of filamentous actin (F-actin) and breast tumor cell invasion assays. In the presence of HA, MDA-MB-231 cells stained with fluorescent phalloidin revealed a significant increase in the assembly of actin fibrils and stress fibers (Fig. 6*A*, *b*). The cytoskeleton reorganization can be observed in MDA-MB-231 cells as early as 30 min following HA addition (Table 1). In the majority of those cells treated with HA for 30 min, the actin filaments were present in numerous stress fibers and/or in thick filaments associated with the plasma membrane and cellular projections as well as perinuclear region (Fig. 6*A*, *b*). Moreover, we have observed that breast tumor cell invasion is also significantly enhanced in cells treated with HA (Table 3, top). In contrast, we found that a small amount of F-actin fragments was randomly distributed in the cytosol in cells not treated with HA (Fig. 6*A*, *a*). Consequently, a very low level of tumor cell invasion was observed in these samples without HA treatment (Table 3, top). The fact that treatment of cells with a ROK inhibitor, Y27632 (Fig. 6*A*, *c*), or a c-Src inhibitor, PP2 (Fig. 6*A*, *c-i*), or anti-CD44 antibody (Fig. 6*A*, *b-i*) followed by HA addition significantly inhibits F-actin formation and tumor cell invasion (Table 3, top) suggests that HA-induced F-actin assembly/reorganization and tumor cell invasion occur in a CD44 and ROK/c-Src-dependent manner. Furthermore, we have noted that stress fibers or actin fibrils were no longer apparent, the total amount of F-actin was greatly reduced, and the disorganized actin was primarily located at the peripheral region of cells treated with miR-10b inhibitor (Fig. 6, *C*, *c*) or Twist siRNA (Fig. 6*B*, *c*) following HA addition. Consequently, cell invasion activity of these cells was also greatly reduced (Table 3, middle and bottom). In contrast, MDA-MB-231 cells treated with an miRNA-negative control (Fig. 6*C*, *a* and *b*) or scrambled siRNA (Fig. 6*B*, *a* and *b*) were capable of inducing F-actin assembly and undergoing tumor cell invasion in the presence of HA (Table 3, middle and bottom) as compared with those cells with no HA treatment. These observations strongly support the contention that HA-mediated CD44 interaction with ROK, c-Src, Twist, and miR-10b signaling is directly involved in the rearrangement of actin filaments/fibers and tumor cell invasion in breast tumor cells.

DISCUSSION

Tumor invasion and metastasis are the primary causes of morbidity in patients diagnosed with solid tumors, such as breast cancer (53). It is now certain that both oncogenic signaling and cytoskeleton functions are directly involved in tumor cell-specific activities, such as tumor cell invasion of surrounding tissue, and metastasis (54, 55). A number of studies have aimed at identifying those molecules that are specifically expressed by epithelial tumor cells and also correlate with metastatic behavior. Among such molecules is HA, a major component in the extracellular matrix of most mammalian tissues. HA is a nonsulfated, unbranched glycosaminoglycan consisting of the repeating disaccharide units D-glucuronic acid and *N*-acetyl-D-glucosamine (56, 57). HA is synthesized by specific HA synthases (57, 58) and digested into various smaller sized molecules by various hyaluronidases (59). HA is enriched in many types of tumors (51, 60). In cancer patients, HA concentrations are generally higher in malignant tumors than in corresponding benign or normal tissues, and in some tumor types, the level of HA is predictive of malignancy (51). In particular,

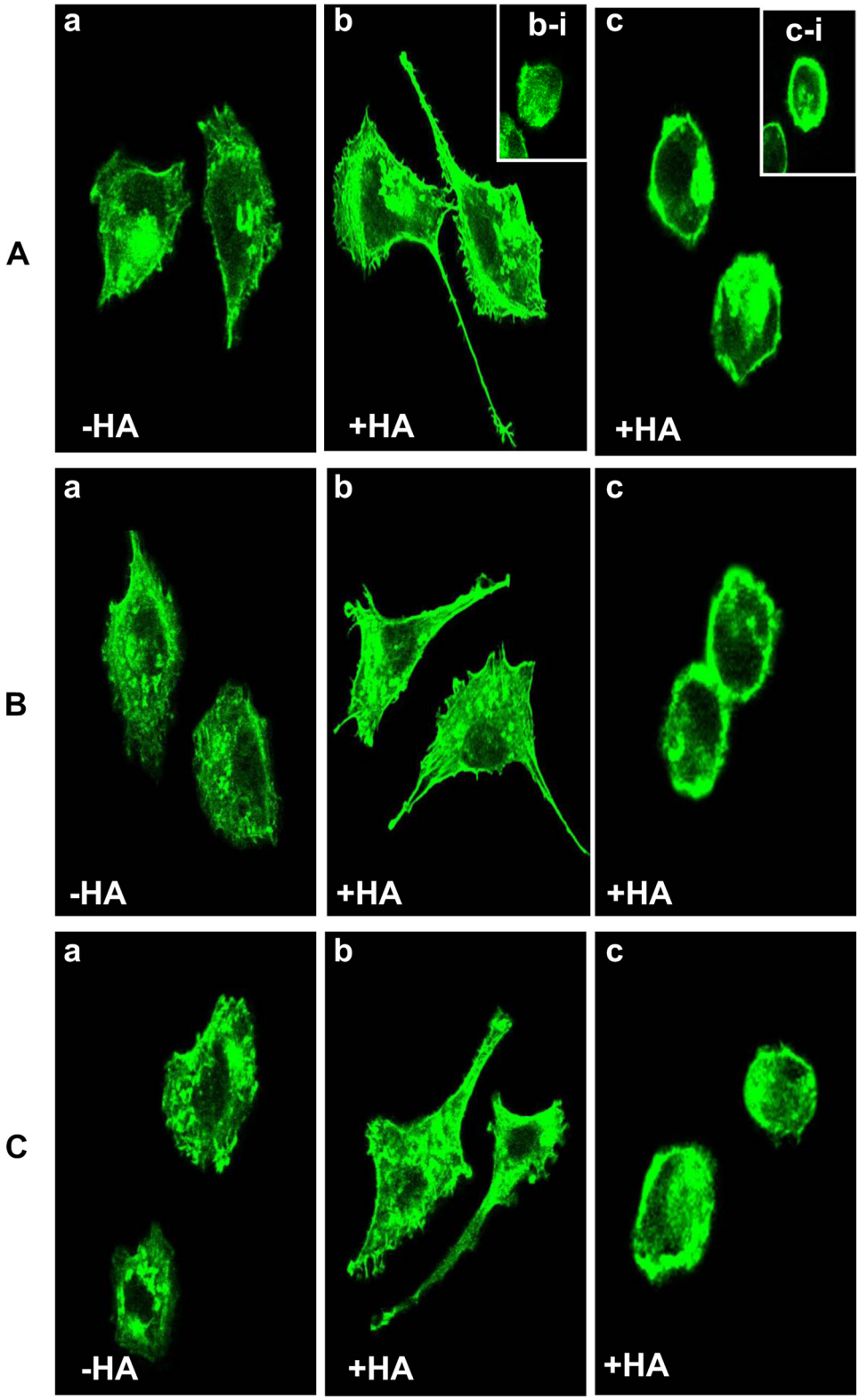

FIGURE 6. **Immunofluorescence staining of F-actin in MDA-MB-231 cells.** MDA-MB-231 cells treated with various agents were fixed by 2% paraformaldehyde. Subsequently, cells were rendered permeable by ethanol treatment and stained with FITC-conjugated phalloidin as described under "Materials and Methods." *A*, localization of FITC-phalloidin-labeled F-actin in MDA-MB-231 cells treated with no HA (*a*) or with HA for 30 min (*b*) or pretreated with anti-CD44 antibody plus 30 min of HA addition (*inset b-i*) or pretreated with Y27632 (*c*) or PP2 (*inset c-i*) for 1 h plus 30 min of HA addition. *B*, localization of FITC-phalloidin-labeled F-actin in cells treated with scrambled siRNA plus no HA (*a*) or with HA for 30 min (*b*) or in cells pretreated with Twist siRNA plus 30 min of HA addition (*c*). *C*, localization of FITC-phalloidin-labeled F-actin in cells treated with miRNA-negative control agent plus no HA (*a*) or with HA for 30 min (*b*) or in cells pretreated with anti-miR-10b inhibitor plus 30 min of HA addition (*c*).

HA levels have been found to be clearly elevated in the serum of breast cancer patients (61).

HA interacts with a specific cell surface receptor, CD44, which belongs to a family of multifunctional transmembrane glycoproteins expressed in numerous cells and tissues, including tumor cells and carcinoma tissues (1–16). The fact that both CD44 and HA are overexpressed at sites of tumor attachment and that HA binding to CD44 stimulates a variety of tumor cell-specific functions and tumor progression (9, 22, 27) suggests that HA-CD44 interaction is a critical requirement for tumor progression. In this study, we have focused specifically on investigating the role of HA-mediated CD44 interaction with unique downstream signaling activators and effectors that coordinate intracellular signaling pathways required for breast tumor cell invasion.

It has been reported that CD44-mediated cellular signaling involves Src kinase family members (62). For example, Lck (one of the Src kinase family members) is found to be closely complexed with CD44 during T-cell activation (62). CD44 also selectively associates with active Src family tyrosine kinases (*e.g.* Lck and Fyn) in glycosphingolipid-rich plasma membrane domains of human peripheral blood lymphocytes (63). Moreover, the cytoplasmic domain of CD44 has been shown to be involved in a complex formation with the Src family (*e.g.* Src, Yes, and Fyn) in prostate tumor cells during anchorage-independent colony growth (2). Collectively, these observations support the notion that c-Src kinases directly participate in CD44-mediated cellular signaling.

In a search for a new c-Src target involved in HA/CD44-mediated tumor invasion and metastasis, we identified the transcription factor Twist. It has been shown that Twist overexpression promotes the epithelial to mesenchymal transition, cell survival, angiogenesis, and chemoresistance *in vitro* (43, 64, 65).

TABLE 3

Measurement of HA-mediated breast tumor cell invasion

Shown are the effects of various agents on HA-induced breast tumor cell invasion (top), the effects of Twist siRNA on HA-mediated breast tumor cell invasion (middle), and the effects of anti-miR-10b inhibitor on HA-mediated breast tumor cell invasion (bottom). All data represent mean ± S.E. (with $n = 5$) of the number of cells undergoing invasion in each sample.

Treatments	Tumor cell invasion (percentage of control)[a]
No treatment (control)	100 ± 5
HA treatment	220 ± 18
HA + anti-CD44 antibody treatment	94 ± 3
HA + PP2 treatment	105 ± 2
HA + Y27632 treatment	102 ± 4

Treatments	Tumor Cell Invasion (percentage of control)	
	Scrambled siRNA-treated cells	Twist siRNA-treated cells
No treatment (control)	100 ± 3	88 ± 3
HA treatment	215 ± 11	82 ± 3

Treatments	Tumor cell invasion (percentage of control)	
	miRNA negative control-treated cells	Anti-miR-10b inhibitor-treated cells
No treatment (control)	100 ± 4	88 ± 3
HA treatment	205 ± 14	82 ± 2

[a] Twenty-four transwell units containing 5-μm porosity polycarbonate filters coated with the reconstituted basement membrane substance Matrigel were used for monitoring *in vitro* tumor cell invasion. Specifically, MDA-MB-231 cells (1×10^4 cells/well untreated or pretreated with anti-CD44 antibody or PP2 (5 μM) or Y27632 (5 μM) or transfected with Twist siRNA or scrambled siRNA or miRNA negative control or anti-miR-10b inhibitor) were placed in the upper chamber of the transwell unit in the presence of 50 μg/ml HA. The growth medium containing high glucose DMEM supplemented by 10% fetal bovine serum was placed in the lower chamber of the transwell unit. After an 18-h incubation at 37 °C in a humidified 95% air, 5% CO_2 atmosphere, cells on the upper side of the filter were removed by wiping with a cotton swab. Cell invasion processes were determined by measuring the cells that migrated to and invaded the lower side of the polycarbonate filters by standard cell number counting methods. The CD44-specific cell invasion was determined by subtracting nonspecific cell invasion (*i.e.* cells that migrated (invaded) to the lower chamber in the presence of anti-CD44 antibody treatment). The CD44-specific cell invasion in untreated cells (Table 2, top, control) or scrambled siRNA-treated cells without HA (Table 2, middle, control) or miRNA negative control-treated cells without HA (Table 2, bottom, control) is designated as 100%. The values expressed in this table represent an average of triplicate determinations of five experiments.

However, the molecular mechanism for Twist involvement in HA/CD44-activated breast cancer cells remains unknown. Here, we have observed that HA-CD44 binding induces the recruitment of c-Src and Twist in MDA-MB-231 cells (Fig. 1). This signaling event then leads to Twist phosphorylation (Fig. 1) and nuclear translocation (Fig. 2), followed by transcriptional activation (Fig. 3) in a c-Src-dependent and CD44-specific manner.

Recently, Twist has gained attention as a putative oncogene that regulates CD44-expressing breast cancer stem cells (44). The binding of Twist to the E-boxes that are located at the promoter regions of many genes (*e.g.* AKT2 and E-cadherin) occurs in breast tumor cells (66, 67). In one example, Twist binding to the E-box elements on the AKT2 promoter enhances transcriptional activity, leading to tumor cell survival and invasiveness in breast cancer cells (66). In another example, Twist interaction with the E-box element of the E-cadherin promoter can transcriptionally repress E-cadherin gene expression in breast cancer (67). Twist overexpression has also been shown to induce miR-10b expression in breast tumor cells (38). However, the molecular mechanism involved in Twist regulation of miR-10b expression has not been fully investigated. In this study, we have found that Twist binds to the E-box-containing promoter of miR-10b and transcriptionally activates miR-10b expression in HA/CD44-treated breast tumor cells (Fig. 3). Down-regulation of c-Src-activated Twist by PP2 and Twist siRNA effectively inhibits HA/CD44-mediated miR-10 expression (Figs. 3 and 4). These findings clearly indicate that Twist is an important upstream activator for miR-10b expression in breast tumor cells following HA-CD44 interaction.

The gene networks orchestrated by many oncogenic miRNAs are still largely unknown, although some key targets have been identified as being involved in breast cancer progression (68, 69). For example, our previous study found that miR-21 can be activated by HA/CD44-activated Nanog-Stat-3 signaling in breast tumor cells, such as the MCF-7 cell line (47). A specific tumor suppressor protein, PDCD4 (program cell death 4) appears to serve as one of the target(s) for miR-21 in breast tumor cells (47). We determined that miR-21 overexpression causes down-regulation of PDCD4 and induces up-regulation of eIF4E, which is a translation initiation factor leading to overexpression of cyclin D1, MDR1 (multidrug-resistant protein)/P-glycoprotein/survivin, and breast tumor cell functions (*e.g.* tumor cell growth, survival, and chemotherapy resistance) (47). To further identify the target(s) affected by HA/CD44-mediated miR-10b function, we focused on HOXD10, a homeobox transcription factor (39). HOXD10 expression has been shown to be progressively reduced in epithelial cells as malignancy increases in breast tumors (38). A previous study also showed that sustained expression of HOXD10 in MDA-MB-231 cells significantly impairs the ability of these breast tumor cells to form tumors in mouse xenografts (70). These findings suggest that HOXD10 functions as a tumor suppressor in mammary epithelial cells (70). In this study, we have demonstrated that HA/CD44-activated c-Src/Twist signaling regulates miR-10b production and HOXD10 down-regulation (Fig. 5), resulting in enhanced expression of RhoGTPases (Fig. 5).

Activated RhoA has been shown to induce membrane protrusion in the epithelial cells (24–27). RhoC, which shares at least 85% sequence homology with RhoA, also participates in the remodeling of the cytoskeleton (24–27, 71, 72). Accumulating evidence suggests that both RhoA and RhoC are critical for breast tumor invasion and/or metastasis (24–27, 71, 72). In particular, a correlation between the invasion activity of different tumor cells and the requirement of RhoA/RhoC-activated signaling has been suggested (24–27, 71, 72). Several different enzymes have been identified as possible downstream targets for RhoA/RhoC signaling. One such enzyme is ROK, which is a serine-threonine kinase known to interact with Rho in a GTP-dependent manner (30, 31). This enzyme has been shown to regulate cytoskeleton function by phosphorylating several important cytoskeletal regulators, including MBS (31), calponin (73), adducin (74), and LIM kinase (75). ROK is also involved in the "cross-talk" between Ras and Rho signaling leading to cellular transformation (76). A previous study also determined that ROK is responsible for the phosphorylation of CD44-associated cytoskeletal proteins during actin filament and plasma membrane interaction. When ROK is overex-

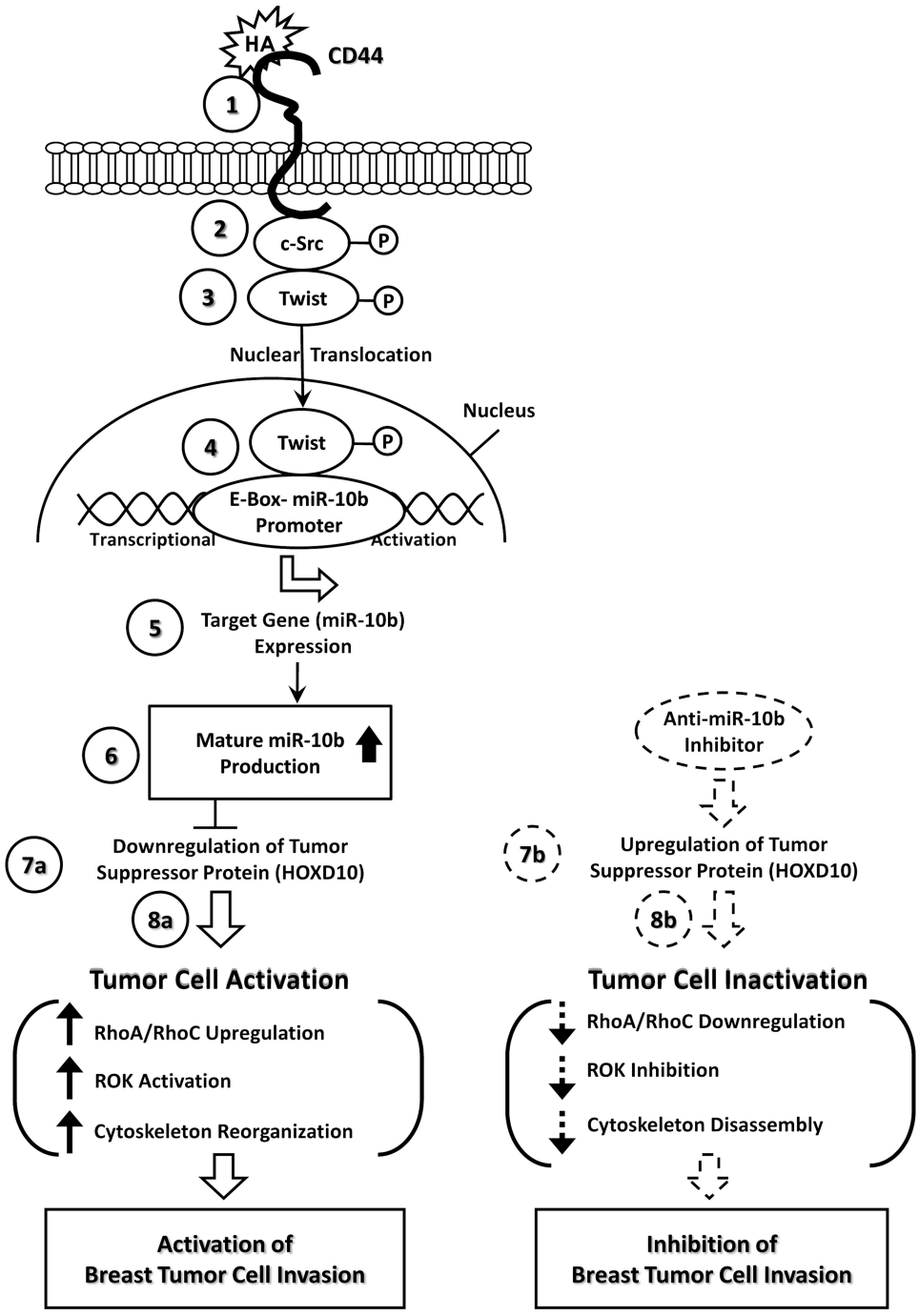

FIGURE 7. **A proposed model for HA/CD44-mediated c-Src activation and Twist signaling in the regulation of miRNA-10b production, HOXD10/RhoGTPase expression, and cytoskeleton function in breast tumor cells.** HA binding to CD44 (*step 1*) promotes c-Src phosphorylation (kinase activation) (*step 2*), which, in turn, causes phosphorylation of Twist (*step 3*). Phosphorylated Twist then translocates from the cytosol to the nucleus and interacts with the E-box elements of mR-10b promoter (*step 4*), resulting in miR-10b gene expression (*step 5*) and mature miR-10b production (*step 6*). The resultant miR-10b then functions to down-regulate the tumor suppressor protein (HOXD10) (*step 7a*) and promotes tumor cell activation (*e.g.* RhoA/RhoC up-regulation, ROK activation, and cytoskeleton reorganization) (*step 8a*), leading to breast tumor cell invasion. In direct contrast, treatment of breast tumor cells with an anti-miR-10b inhibitor induces tumor suppressor protein (HOXD10) up-regulation (*step 7b*; indicated by the *arrow* with *dashed lines*). Subsequently, these changes result in tumor cell inactivation, including down-regulation of RhoGTPase (RhoA/RhoC) expression (*step 8b*; indicated by the *arrow* with *dashed lines*) and inhibition of ROK-cytoskeleton functions (*e.g.* tumor cell invasion) (*step 8b*; indicated by the *arrow* with *dashed lines*) in breast tumor cells.

pressed or constitutively activated, changes in actin cytoskeleton organization occur that are similar to those observed during normal Rho-activated conditions (31). ROK is overexpressed in breast tumor cells and is capable of phosphorylating the cytoplasmic domain of CD44 (11). Moreover, phosphorylation of the cytoplasmic domain of CD44 by ROK enhances its binding interaction with the cytoskeletal protein ankyrin (11). Overexpression of the Rho-binding domain (a dominant negative form) of ROK by transfecting breast tumor cells with RB cDNA induces reversal of tumor cell-specific phenotypes (11). These findings support the notion that ROK plays a pivotal role in CD44-cytoskeleton interaction and Rho-mediated oncogenic signaling required for membrane-cytoskeleton function and metastatic tumor cell migration. In this study, we have found that down-regulation of HA/CD44-activated c-Src/Twist signaling (by PP2/Twist siRNA) and miR-10b production (by anti-miR-10b inhibitor) not only induces HOXD10 up-regulation (Fig. 5) but also inhibits the expression of RhoGTPases (*e.g.* RhoA and RhoC) (Fig. 5). Subsequently, these signaling perturbation events contribute to inhibition of ROK activity and impairment of cytoskeleton organization (Fig. 6), ROK activity, and tumor cell invasion (Tables 2 and 3). These findings clearly establish causal links between c-Src/Twist signaling and miR-10b function, including HOXD10 down-regulation, and RhoGTPase-associated cytoskeleton activation.

As summarized in Fig. 7, we propose that HA binding to CD44 (*step 1*) promotes c-Src phosphorylation (kinase activation) (*step 2*), which, in turn, causes phosphorylation of Twist (*step 3*). Phosphorylated Twist then translocates from the cytosol to the nucleus and interacts with the E-box elements of the mR-10b promoter (*step 4*), resulting in miR-10b gene expression (*step 5*) and mature miR-10b production (*step 6*). The resultant miR-10b then functions to down-regulate the tumor suppressor protein (HOXD10) (*step 7a*) and promotes tumor cell activation (*e.g.* RhoA/RhoC up-regulation, ROK activation, and cytoskeleton reorganization) (*step 8a*), leading to breast tumor cell invasion. In direct contrast, treatment of breast tumor cells

with an anti-miR-10b inhibitor induces tumor suppressor protein (HOXD10) up-regulation (*step 7b*). Subsequently, these changes result in tumor cell inactivation, including down-regulation of RhoGTPase (RhoA/RhoC) expression and inhibition of ROK-cytoskeleton functions (*e.g.* tumor cell invasion) (*step 8b*) in breast tumor cells. In recent years, compelling evidence has accumulated that tumor invasion and metastasis can be initiated by miR-10b in breast cancer (38). Thus, the results of this study elucidating the HA/CD44 signaling pathway-specific mechanisms involved in miR-10b production are significant for the formulation of future intervention strategies in the treatment of breast cancer invasion and/or metastasis.

Acknowledgments—We gratefully acknowledge the assistance of Drs. Gerard J. Bourguignon and Walter M. Holleran in the preparation and review of the manuscript. We are grateful to Christina Camacho for assistance in preparing the figures.

REFERENCES

1. Iida, N., and Bourguignon, L. Y. (1995) *J. Cell. Physiol.* **162,** 127–133
2. Zhu, D., and Bourguignon, L. Y. W. (1998) *Cell Motil. Cytoskeleton* **39,** 209–222
3. Iida, N., and Bourguignon, L. Y. (1997) *J. Cell. Physiol.* **171,** 152–160
4. Bourguignon, L. Y., Zhu, H., Chu, A., Iida, N., Zhang, L., and Hung, M. C. (1997) *J. Biol. Chem.* **272,** 27913–27918
5. Günthert, U., Hofmann, M., Rudy, W., Reber, S., Zöller, M., Haussmann, I., Matzku, S., Wenzel, A., Ponta, H., and Herrlich, P. (1991) *Cell* **65,** 13–24
6. Auvinen, P., Tammi, R., Tammi, M., Johansson, R., and Kosma, V. M. (2005) *Histopathology* **47,** 420–428
7. Bourguignon, L. Y. (2001) *J. Mammary Gland Biol. Neoplasia* **6,** 287–297
8. Bourguignon, L. Y., Zhu, D., and Zhu, H. (1998) *Front. Biosci.* **3,** D637–649
9. Turley, E. A., Noble, P. W., and Bourguignon, L. Y. (2002) *J. Biol. Chem.* **277,** 4589–4592
10. Bourguignon, L. Y., Gunja-Smith, Z., Iida, N., Zhu, H. B., Young, L. J., Muller, W. J., and Cardiff, R. D. (1998) *J. Cell. Physiol.* **176,** 206–215
11. Bourguignon, L. Y., Zhu, H., Shao, L., Zhu, D., and Chen, Y. W. (1999) *Cell Motil. Cytoskeleton* **43,** 269–287
12. Bourguignon, L. Y., Singleton, P. A., Zhu, H., and Diedrich, F. (2003) *J. Biol. Chem.* **278,** 29420–29434
13. Bourguignon, L. Y., Zhu, H., Shao, L., and Chen, Y. W. (2000) *J. Biol. Chem.* **275,** 1829–1838
14. Bourguignon, L. Y., Zhu, H., Zhou, B., Diedrich, F., Singleton, P. A., and Hung, M. C. (2001) *J. Biol. Chem.* **276,** 48679–48692
15. Bourguignon, L. Y., Zhu, H., Shao, L., and Chen, Y. W. (2001) *J. Biol. Chem.* **276,** 7327–7336
16. Bourguignon, L. Y., Singleton, P. A., Zhu, H., and Zhou, B. (2002) *J. Biol. Chem.* **277,** 39703–39712
17. Screaton, G. R., Bell, M. V., Jackson, D. G., Cornelis, F. B., Gerth, U., and Bell, J. I. (1992) *Proc. Natl. Acad. Sci. U.S.A.* **89,** 12160–12164
18. Al-Hajj, M., Wicha, M. S., Benito-Hernandez, A., Morrison, S. J., and Clarke, M. F. (2003) *Proc. Natl. Acad. Sci. U.S.A.* **100,** 3983–3988
19. Haylock, D. N., and Nilsson, S. K. (2006) *Regen. Med.* **1,** 437–445
20. Summy, J. M., and Gallick, G. E. (2003) *Cancer Metastasis Rev.* **22,** 337–358
21. Schlessinger, J. (2000) *Cell* **100,** 293–296
22. Bourguignon, L. Y. (2009) in *Hyaluronan in Cancer Biology* (Stern, R., ed) pp. 89–101, Academic Press, Inc., New York
23. Hall, A. (1998) *Science* **279,** 509–514
24. Li, X., and Lim, B. (2003) *Oncol. Res.* **13,** 323–331
25. Fritz, G., Just, I., and Kaina, B. (1999) *Int. J. Cancer* **81,** 682–687
26. Suwa, H., Ohshio, G., Imamura, T., Watanabe, G., Arii, S., Imamura, M., Narumiya, S., Hiai, H., and Fukumoto, M. (1998) *Br. J. Cancer* **77,** 147–152
27. Bourguignon, L. Y. W. (2008) *Semin. Cancer Biol.* **18,** 251–259
28. Singleton, P. A., and Bourguignon, L. Y. (2002) *Cell Motil. Cytoskeleton* **53,** 293–316
29. Bourguignon, L. Y., Singleton, P. A., Diedrich, F., Stern, R., and Gilad, E. (2004) *J. Biol. Chem.* **279,** 26991–27007
30. Amano, M., Ito, M., Kimura, K., Fukata, Y., Chihara, K., Nakano, T., Matsuura, Y., and Kaibuchi, K. (1996) *J. Biol. Chem.* **271,** 20246–20249
31. Kimura, K., Ito, M., Amano, M., Chihara, K., Fukata, Y., Nakafuku, M., Yamamori, B., Feng, J., Nakano, T., Okawa, K., Iwamatsu, A., and Kaibuchi, K. (1996) *Science* **273,** 245–248
32. Amano, M., Chihara, K., Kimura, K., Fukata, Y., Nakamura, N., Matsuura, Y., and Kaibuchi, K. (1997) *Science* **275,** 1308–1311
33. Vasudevan, S., Tong, Y., and Steitz, J. A. (2007) *Science* **318,** 1931–1934
34. Calin, G. A., and Croce, C. M. (2006) *Cancer Res.* **66,** 7390–7394
35. Ma, L., and Weinberg, R. A. (2008) *Cell Cycle* **7,** 570–572
36. Sasayama, T., Nishihara, M., Kondoh, T., Hosoda, K., and Kohmura, E. (2009) *Int. J. Cancer* **125,** 1407–1413
37. Tian, Y., Luo, A., Cai, Y., Su, Q., Ding, F., Chen, H., and Liu, Z. (2010) *J. Biol. Chem.* **285,** 7986–7994
38. Ma, L., Teruya-Feldstein, J., and Weinberg, R. A. (2007) *Nature* **449,** 682–688
39. Ma, L., Reinhardt, F., Pan, E., Soutschek, J., Bhat, B., Marcusson, E. G., Teruya-Feldstein, J., Bell, G. W., and Weinberg, R. A. (2010) *Nat. Biotechnol.* **28,** 341–347
40. Jan, Y. N., and Jan, L. Y. (1993) *Proc. Natl. Acad. Sci. U.S.A.* **90,** 8305–8307
41. Murre, C., McCaw, P. S., and Baltimore, D. (1989) *Cell* **56,** 777–783
42. Cheng, G. Z., Zhang, W. Z., Sun, M., Wang, Q., Coppola, D., Mansour, M., Xu, L. M., Costanzo, C., Cheng, J. Q., and Wang, L. H. (2008) *J. Biol. Chem.* **283,** 14665–14673
43. Yang, J., Mani, S. A., Donaher, J. L., Ramaswamy, S., Itzykson, R. A., Come, C., Savagner, P., Gitelman, I., Richardson, A., and Weinberg, R. A. (2004) *Cell* **117,** 927–939
44. Vesuna, F., Lisok, A., Kimble, B., and Raman, V. (2009) *Neoplasia* **11,** 1318–1328
45. Bourguignon, L. Y., Peyrollier, K., Xia, W., and Gilad, E. (2008) *J. Biol. Chem.* **283,** 17635–17651
46. Bourguignon, L. Y., Xia, W., and Wong, G. (2009) *J. Biol. Chem.* **284,** 2657–2671
47. Bourguignon, L. Y., Spevak, C. C., Wong, G., Xia, W., and Gilad, E. (2009) *J. Biol. Chem.* **284,** 26533–26546
48. Zhou, X., Ruan, J., Wang, G., and Zhang, W. (2007) *PLoS Comput. Biol.* **3,** e37
49. Torre, C., Wang, S. J., Xia, W., and Bourguignon, L. Y. (2010) *Arch. Otolaryngol. Head Neck Surg.* **136,** 493–501
50. Tammi, M. I., Day, A. J., and Turley, E. A. (2002) *J. Biol. Chem.* **277,** 4581–4584
51. Toole, B. P., Wight, T. N., and Tammi, M. I. (2002) *J. Biol. Chem.* **277,** 4593–4596
52. Osusky, M., Taylor, S. J., and Shalloway, D. (1995) *J. Biol. Chem.* **270,** 25729–25732
53. Parker, B., and Sukumar, S. (2003) *Cancer Biol. Ther.* **2,** 14–21
54. Jiang, W. G., Puntis, M. C., and Hallett, M. B. (1994) *Br. J. Surg.* **81,** 1576–1590
55. Lauffenburger, D. A., and Horwitz, A. F. (1996) *Cell* **84,** 359–369
56. Laurent, T. C., and Fraser, J. R. (1992) *FASEB J.* **6,** 2397–2404
57. Lee, J. Y., and Spicer, A. P. (2000) *Curr. Opin Cell Biol.* **12,** 581–586
58. Toole, B. P. (2001) *Semin. Cell Dev. Biol.* **12,** 79–87
59. Stern, R., and Jedrzejas, M. J. (2006) *Chem. Rev.* **106,** 818–839
60. Knudson, W., Biswa, C., Li, X., Nemec, R. E., and Toole, B. P. (1989) *Ciba Found. Symp.* **143,** 150–159
61. Delpech, B., Chevallier, B., Reinhardt, N., Julien, J. P., Duval, C., Maingonnat, C., Bastit, P., and Asselain, B. (1990) *Int. J. Cancer* **46,** 388–390
62. Taher, T. E., Smit, L., Griffioen, A. W., Schilder-Tol, E. J., Borst, J., and Pals, S. T. (1996) *J. Biol. Chem.* **271,** 2863–2867
63. Ilangumaran, S., Briol, A., and Hoessli, D. C. (1998) *Blood* **91,** 3901–3908
64. Yuen, H. F., Chan, Y. P., Wong, M. L., Kwok, W. K., Chan, K. K., Lee, P. Y., Srivastava, G., Law, S. Y., Wong, Y. C., Wang, X., and Chan, K. W. (2007) *J. Clin. Pathol.* **60,** 510–514

65. Pham, C. G., Bubici, C., Zazzeroni, F., Knabb, J. R., Papa, S., Kuntzen, C., and Franzoso, G. (2007) *Mol. Cell. Biol.* **27,** 3920–3935
66. Cheng, G. Z., Chan, J., Wang, Q., Zhang, W., Sun, C. D., and Wang, L. H. (2007) *Cancer Res.* **67,** 1979–1987
67. Vesuna, F., van Diest, P., Chen, J.. H., and Raman, V. (2008) *Biochem. Biophys. Res. Commun.* **367,** 235–241
68. O'Day, E., and Lal, A. (2010) *Breast Cancer Res.* **12,** 201
69. Baffa, R., Fassan, M., Volinia, S., O'Hara, B., Liu, C. G., Palazzo, J. P., Gardiman, M., Rugge, M., Gomella, L. G., Croce, C. M., and Rosenberg, A. (2009) *J. Pathol.* **219,** 214–221
70. Carrio, M., Arderiu, G., Myers, C., and Boudreau, N. J. (2005) *Cancer Res.* **65,** 7177–7185
71. Wu, M., Wu, Z. F., Rosenthal, D. T., Rhee, E. M., and Merajver, S. D. (2010) *Cancer* **116,** 2768–2782
72. Wu, D., Asiedu, M., and Wei, Q. (2009) *Oncogene* **28,** 2219–2230
73. Kaneko, T., Amano, M., Maeda, A., Goto, H., Takahashi, K., Ito, M., and Kaibuchi, K. (2000) *Biochem. Biophys. Res. Commun.* **273,** 110–116
74. Fukata, Y., Oshiro, N., Kinoshita, N., Kawano, Y., Matsuoka, Y., Bennett, V., Matsuura, Y., and Kaibuchi, K. (1999) *J. Cell Biol.* **145,** 347–361
75. Amano, T., Tanabe, K., Eto, T., Narumiya, S., and Mizuno, K. (2001) *Biochem. J.* **354,** 149–159
76. Sahai, E., Olson, M. F., and Marshall, C. J. (2001) *EMBO J.* **20,** 755–766